THE UNIVERSITY OF CALGARY

Investigation of Mitotically-Active Cells in the Adult Mouse Hippocampus

by

Rodney Rietze

A THESIS

SUBMITTED TO THE FACULTY OF GRADUATE STUDIES

IN PARTIAL FULFILLMENT OF THE REQUIREMENTS FOR THE

DEGREE OF MASTER OF SCIENCE

DEPARTMENT OF NEUROSCIENCE

CALGARY, ALBERTA

SEPTEMBER, 1996

ABSTRACT

Previous studies of the adult rat hippocampus have reported neurogenesis in the region of the dentate gyrus. In the present work, a novel labeling protocol was developed in an attempt to account for the cytokinetic changes in cell turnover which occur in the central nervous system as an animal ages. Following the adminstration of intraperitoneal injections of bromodeoxyuridine every two hours for a period of 48 hours, mitotically-active cells were identified in the dentate gyrus of the adult mouse. However, mitotically-active cells were also observed throughout Ammon's horn. Studies of the number and distribution of mitotically-active cells, comparing the bromodeoxyuridine protocol with an identical protocol employing lower concentrations of tritiated thymidine, suggest a lack of toxicity in long term labeling. Immunocytochemical analysis of the bromodeoxyuridine-immunoreactive cells immediately following the labeling period, showed a lack of antigenic expression of known markers for neurons and astrocytes. Subsequent analysis of the cells' antigenic properties performed at 3, 6, 9, 12, and 24 weeks demonstrated the presence of double-labeled glia and neurons throughout the hippocampus. These results demonstrate for the first time, the generation of new neurons and glia in Ammon's horn of the adult hippocampus. The distribution of the newly-generated cells suggests that they may participate in the modulation of synaptic efficacy.

ACKNOWLEDGMENTS

I would like to thank Dr. Sam Weiss for all the time and effort he contributed to this project, and his encouraging me to strive for excellence. I have learned a lot Sam. I would also like to thank Christine Dunne and Chris Bjornson for their support and encouragement. You both helped me to continue when I thought I could not. I am indebted to each member of my examination committee for their unique insights into this work, but especially so to Dr. Poulin . . . thank you for everything Paule. Finally, I must thank my wife Jacquie. Your quiet endurance and support through the long hours and late nights did not go unnoticed.

To the One who knows

Silver or gold I do not have, but what I have I give to you.

TABLE OF CONTENTS

LIST OF FIGURES

LIST OF ABBREVIATIONS

Anatomy

CNS	central nervous system
DG	dentate gyrus
Dge	external dentate limb
dgm 1	first dentate migration
dgm 2	second dentate migration
dgt	tertiary dentate matrix
FI	fimbria
Gr	granule cell layer of the dentate gyrus
h	hilus of the dentate gyrus
Inf	infrapyramidal limb of the dentate gyrus
Lmol	lacunosum moleculare of Ammon's horn
Mol	stratum moleculare of the dentate gyrus
ne	hippocampal neuroepithelium
Or	oriens layer
Py	pyramidal cell layer
S-phase	synthesis phase
Sb	subiculum
sgz	subgranular zone
Sup	suprapyramidal layer of the denate gyrus
3rd	third ventricle

Other Terms

B.W.	body weight
BrdU	Bromodeoxyuridine
DNA	deoxyribonucleic acid
E	embryonic day
FITC	fluorescein isothiocynate
GABA	gamma aminobutryic acid
GFAP	glial fibrillary acidic protien
[^{3}H]	tritiated
hrs	hours
IgG	immunoglobulin G
i.p.	intraperitoneal
IR	Immunoreactive
P	post-natal day
PBS	phosphate buffered saline

1. INTRODUCTION

The hippocampal formation is one of the most intensely studied and well described regions in the mammalian central nervous system (CNS). Its characteristics have been the focus of numerous investigations since Ramón y Cajal (1911) and his pupil, Lorente de Nó (1934), performed their historic Golgi studies. Interest in the hippocampus is warranted not only through its functional role in learning and memory (Alkon *et al.* , 1991; Squire, 1992; Zola-Morgan and Squire, 1993), but also by the unique organizational and developmental characteristics it possesses. Its highly ordered structure and extended period of neurogenesis have made the hippocampus a popular model for the study of brain plasticity and regenerative capacity (reviewed in Isaacson and Pribram, 1975, 1985).

1.1 *Structural organization of the hippocampus*

Compared to other regions of the CNS, the hippocampus is characterized by a relatively simple cytoarchitecture. In a coronal section, the hippocampus has an appearance of two arcs (Figure 1), the smaller one (dentate gyrus) bordering on the inferior edge of the larger arc (Ammon's horn). The large arc of Ammon's horn is composed of a narrow layer (3-5 cells deep) of pyramidal cells divided into 4 fields; CA1, CA2, CA3, and CA4 which extend from the subiculum (Sb), towards the dentate gyrus (Lorente de Nó, 1934; Blackstad,

Figure 1. A coronal section of the hippocampal region in an adult mouse.

This cresyl violet stained coronal section (14 μm) of the adult mouse hippocampus corresponds closely to Plate 42 of the stereotaxic atlas of Sidman *et al.* (1971), at a level about -1.3 bregma. Abbreviations: *DG*, dentate gyrus; *Gr*, granule cell layer of the dentate gyrus; *h* , hilus of the dentate gyrus (also called CA4); *Inf*, infrapyramidal limb of the dentate granular layer; *Lmol*, lacunosum moleculare layer of Ammon's horn; *Mol*, stratum moleculare of the dentate gyrus; *Or*, oriens layer; *Py*, pyramidal cell layer; *Rad*, radiatum layer; *Sb*, subiculum; *Sup*, suprapyramidal limb of the dentate granular layer; 3^{rd}, third ventricle. Figure adapted from Slotnick and Leonard (1975).

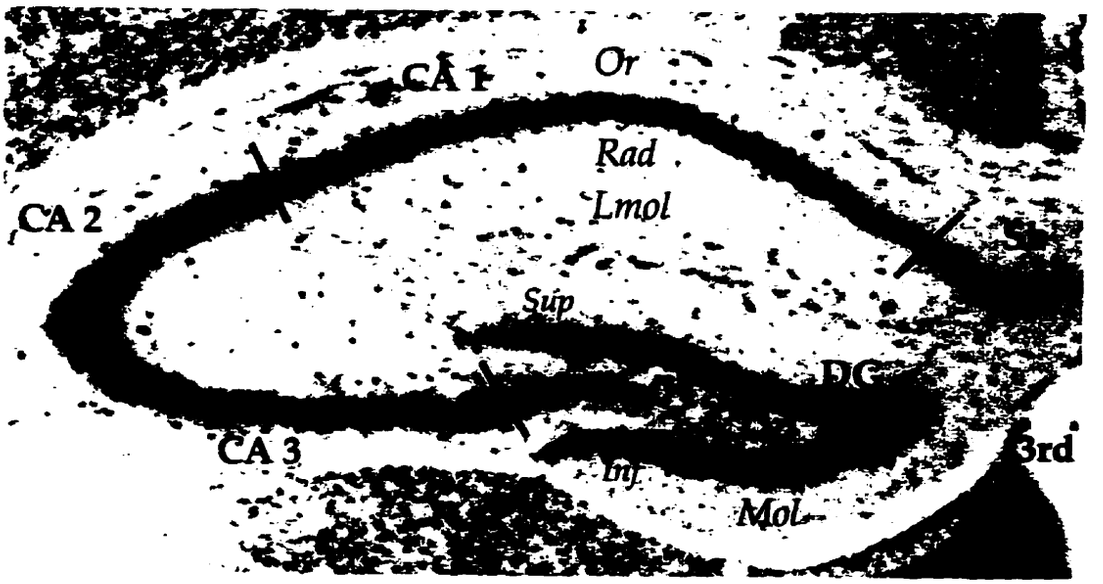
CA 1
Or
Rad
Lmol
CA 2
Sup
DG
CA 3
3rd
Inf
Mol

1956; Angevine, 1965). The CA1 region is immediately adjacent to the subiculum and is composed of tightly packed medium-sized cells. Following CA1 (solid line in Fig. 1), a field of larger, less densely packed cells (CA2 and CA3) are apparent (reviewed in Schwerdtfeger, 1984). (In Nissl stained sections the CA2 region can not be accurately distinguished from CA3, therefore they will be considered one region (CA2-3) for the purposes of this study).

Finally, as the pyramidal cell layer extends towards the region of the dentate gyrus it begins to increase in cell density and volume. It is this increase (solid line in Figure 1) which defines the boundary between CA3 and CA4 fields. Lorente de Nó (1934), originally classified the CA4 region as a part of Ammon's horn, however, since the region contains polymorph, fusiform, and other modified pyramidal cell types many today consider it a part of the dentate gyrus calling it the hilar region (h) (Amaral, 1978; Swanson *et al.* , 1978; Schwerdtfeger, 1984). For the purposes of this study the more recent classification will be followed. It should be noted that the demarcation employed in Figure 1 is not absolute, but rather reflects operational boundaries through which cell counts are realized.

The small arc of the dentate gyrus is composed of densely packed (4- 10 cells deep) granule cells which are divided into two limbs or blades (reviewed in Cowan *et al.* , 1980; Bayer, 1985). The dorsal limb, which is closest to the hippocampal fissure, is called the suprapyramidal (Sup), and the other limb the

infrapyramidal (Inf) in reference to their relative positions to stratum pyramidal of Ammon's horn (Isaacson, 1987).

1.2 Hippocampal cell types

The dominant neuronal cell types of the hippocampus are the pyramidal cells of Ammon's horn, and the granular cells of the dentate gyrus. Dentate granular cells are relatively small in diameter (~8-12μm) in comparison to pyramidal cells (~15-20μm) (Bayer, 1985). All of the cells in the granule cell layer are uniformly orientated such that their dendrites extend vertically from the superficial aspect of the cells towards the molecular layer (Mol) (Anderson, 1975; Stanfield and Cowan, 1979a; Braitenberg and Schuz, 1983; Amaral and Witter, 1989). The pyramidal cells of Ammon's horn are also uniformly orientated such that their apical dendrites extend into stratum radiatum and lacunosum moleculare layers, while the basal dendrites exit into the oriens layer (Lorente de Nó, 1934; Blackstad, 1956; Angevine, 1965, 1975; Laurberg, 1979; Bannister and Larkman, 1995 a, b).

Within the concavity of the granule cell layer (i.e. hilus) are several layers of polymorphic neurons. Classically, these neurons have been characterized as basket, chandelier, mossy, GABAergic, peptidergic, and modified pyramidal cell types based on their typical morphology and neurochemical content (Lorente de Nó, 1934; Blackstad, 1956; Angevine, 1965, 1975; Isaacson, 1975; Laurberg, 1979). However the classifications are by no means exhaustive of the diversity

of neuronal cell types found within the region. It is believed that the polymorphic region within the dentate is a continuation of stratum oriens of Ammon's horn, since it exhibits cell types similar to that of stratum oriens. The majority of the polymorph cells are thought to function as interneurons, both within the region of the dentate gyrus and within Ammon's horn (reviewed in Schwerdtfeger, 1984).

Within the CA1 region of Ammon's horn, three types of interneurons or local circuit neurons are of relevance to this study: basket cells, oriens/alveus (O/A) interneurons, and lacunosum-moleculare (L-M) interneurons. Basket cells received their name because of the "basket-like" axonal plexus around the cell bodies of pyramidal cells (Lacaille *et al.*, 1989). Basket cells are characterized by large somas (approximately 45 μm in diameter) and the presence of basal and apical dendrites (Lorente de Nó, 1934). Most of these cells are considered to be GABAergic inhibitory interneurons, which receive synaptic input from a variety of sources (Schwartzkroin and Mathers, 1978; Ashwood *et al.*, 1984). O/A interneurons are multipolar cells, 20-30μm in diameter, located on the oriens-alveus border. The majority of their dendrites run parallel to the alveus, and receive numerous synaptic contacts (Lacaille *et al.*, 1989). Like the basket cells, O/A neurons appear to be GABAergic in nature. L-M interneurons are located within the lacunosum-moleculare region of CA1, and are characterized by extensive dendritic and axonal projections (dendritic trees span two-thirds of

CA1 and part of the dentate gyrus) (Kunkel *et al.*, 1988). Their axons also branch extensively with processes reaching as far as stratum oriens. As with basket and O/A interneurons, L-M interneurons are inhibitory in nature.

The distribution of glia within the hippocampus generally corresponds to the laminar organization and afferent fiber orientation in the particular region (Rose *et al.* , 1976; Gall *et al.* , 1979; Zimmer and Sunde, 1984; Kosaka and Hama, 1986). As a result, in Ammon's horn each neuropil layer is characterized by it's own astroglial cytoarchitecture, while in the dentate astrocyte cell bodies are vertically orientated into the granular layer, corresponding to the granule cells fiber orientations there.

1.3 *Development of the hippocampus*

The principle data concerning the sequence of events in the development of the hippocampus were obtained in autoradiographic experiments by administering tritiated ([^{3}H])-thymidine to a series of pregnant animals or directly to their offspring. Thymidine, a specific precursor of chromosomal deoxyribonucleic acid (DNA), is incorporated into cell nuclei during the S-phase of the cell cycle, when new DNA is being formed (Taylor *et al.*, 1957; Hughes *et al.*, 1958; Sidman *et al.*, 1959). When animals are injected with [^{3}H]-thymidine only the cells proliferating at the time of the injection tend to incorporate the administered nucleotide and become "tagged". By harvesting the brains of

groups of animals at different times after the administration of the radiolabel, a time-lapse record can be established, mapping the fate of the tagged cells in regards to their subsequent divisions, migrations, and differentiations. Such investigations performed in the mouse (Angevine, 1965; Atlas and Bond, 1965; Caviness, 1973; Stanfield and Cowan, 1979b; Reznikov, 1991), rat (Altman and Das, 1965; Bayer and Altman, 1974, 1975; Schlessinger *et al.* , 1975; Kaplan and Hinds, 1977; Bayer, 1980a, 1982; Bayer *et al.*, 1993), rabbit (Fernandez, 1969; Fernandez and Bravo, 1974; Gueneau *et al.*, 1982), guinea pig (Altman and Das, 1967), cat (Altman, 1963; Wyss and Sripanidkulchai, 1985), and rhesus monkey (Rakic and Nowakowski, 1981; Nowakowski and Rakic, 1981; Rakic, 1985a, b; Eckenhoff and Rakic, 1988) revealed that while the duration of neurogenesis was not the same, the overall sequence of hippocampal neurogenesis was conserved in all mammals. This sequence of neurogenesis (in the rat) is presented schematically in Figures 2 and 3.

In the rat hippocampus, the generation of neurons begins on embryonic (E) day 15. The large neurons of the supra- and infrapyramidal regions of Ammon's horn are generated first (E15-E17), followed by the pyramidal neurons between E17 and E19 (Bayer and Altman, 1974; Hine and Das, 1974; Bayer, 1980 a, b; Altman and Bayer, 1990 a, b). Neurogenesis in the dentate gyrus follows the same pattern, with the production of neurons in the molecular and hilar regions (E15-E19) preceding the production of granular neurons (E17) (Bayer and Altman, 1974; Bayer, 1980 a, b; Altman and Bayer, 1990 a, c). While the onset of

Figure 2. Morphogenetic migrations in the development of Ammon's horn.

Neurogenesis begins on embryonic (E) day 15 with a high level of proliferative activity within the hippocampal neuroepithelium (*ne*). The pyramidal cells (those of the CA3 region) close to the fimbria (*FI*), are generated first (peaking at E17), extending the neuroepithelium towards the subiculum (*SU*). The pyramidal neurons closer to the *SU*, (those of CA1), are subsequently generated much later (peaking on E18), but settle in stratum pyramidale before the earlier generated CA3 cells (see *CA1m* at plate *E20*). So, early-generated pyramidal cells are destined to settle in the late forming CA3 region, while late-generated pyramidal cells are destined to settle in the early-forming CA1 region. Figure taken from Altman and Bayer (1990b).

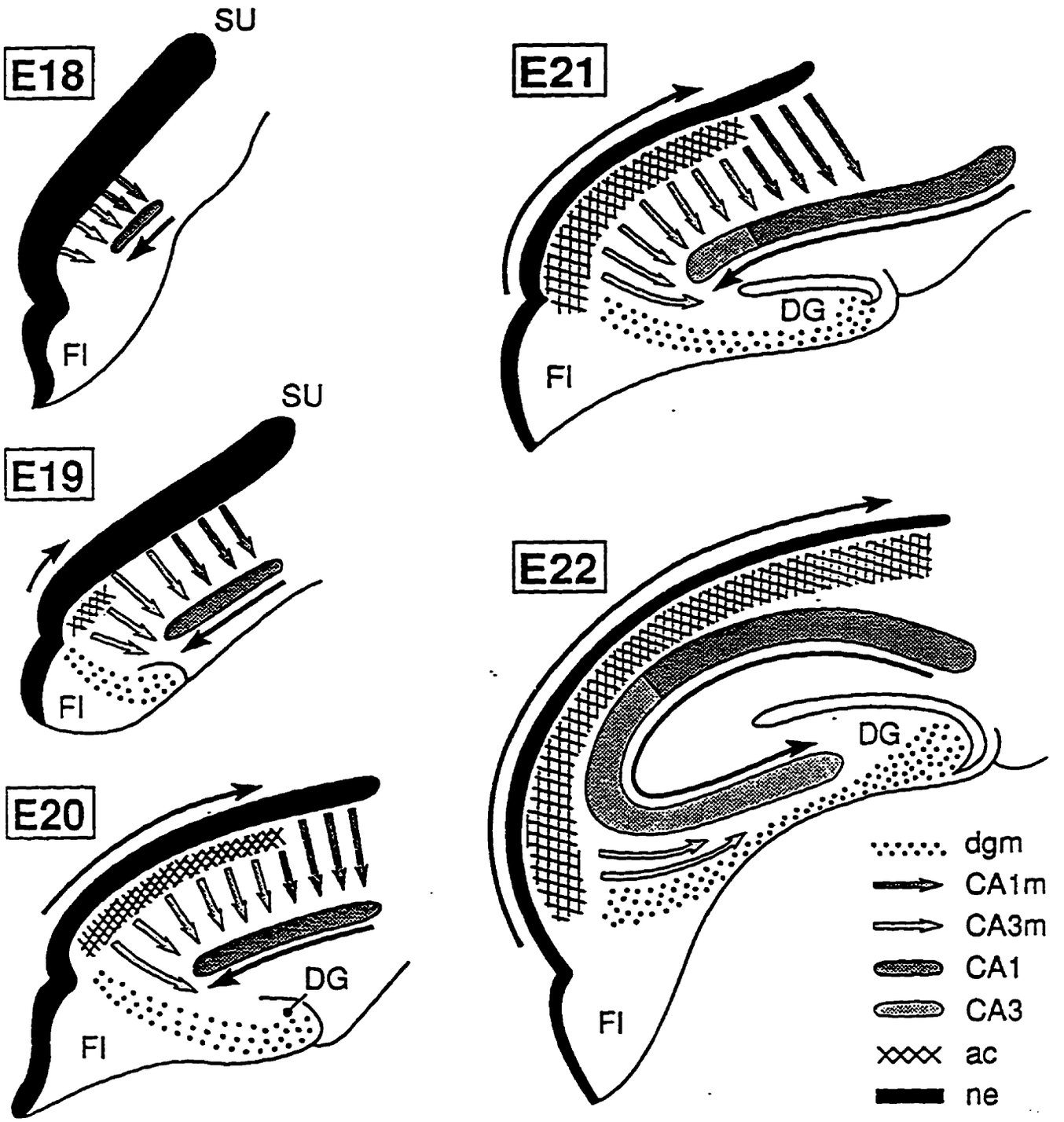
E18
SU
Fl
E19
SU
Fl
E20
DG
Fl
E21
DG
Fl
E22
DG
Fl
dgm
CA1m
CA3m
CA1
CA3
ac
ne

Figure 3. Morphogenetic migrations in the development of the dentate gyrus.

Beginning on day E19, proliferating cells of the secondary dentate matrix proceed toward the developing dentate gyrus, forming the dentate migration. The first dentate migration (*dgm 1*) is the source of the earliest generated granule cells that will later constitute the outer shell, or skeleton, of the granular layer. The second dentate migration (*dgm 2*) penetrates the basal polymorph layer and reaches the tip of the external dentate limb (*DGe*) by the first few days after birth. The second dentate migration gives rise in succession to the transient tertiary dentate matrix(*dgt*) and the enduring subgranular zone (*sgz*). These two germinal matrices represent the intrinsic (intradentate) sources of the large compliment of postnatally acquired "late" and "latest" granule cells that settle in the inner core of the granular layer immediately above the subgranular zone. The tertiary dentate matrix is prominent between days P3 and P10, after which its cells settle into the region of the subgranular zone to form a continuous proliferative matrix. Figure taken from Altman and Bayer (1990c).

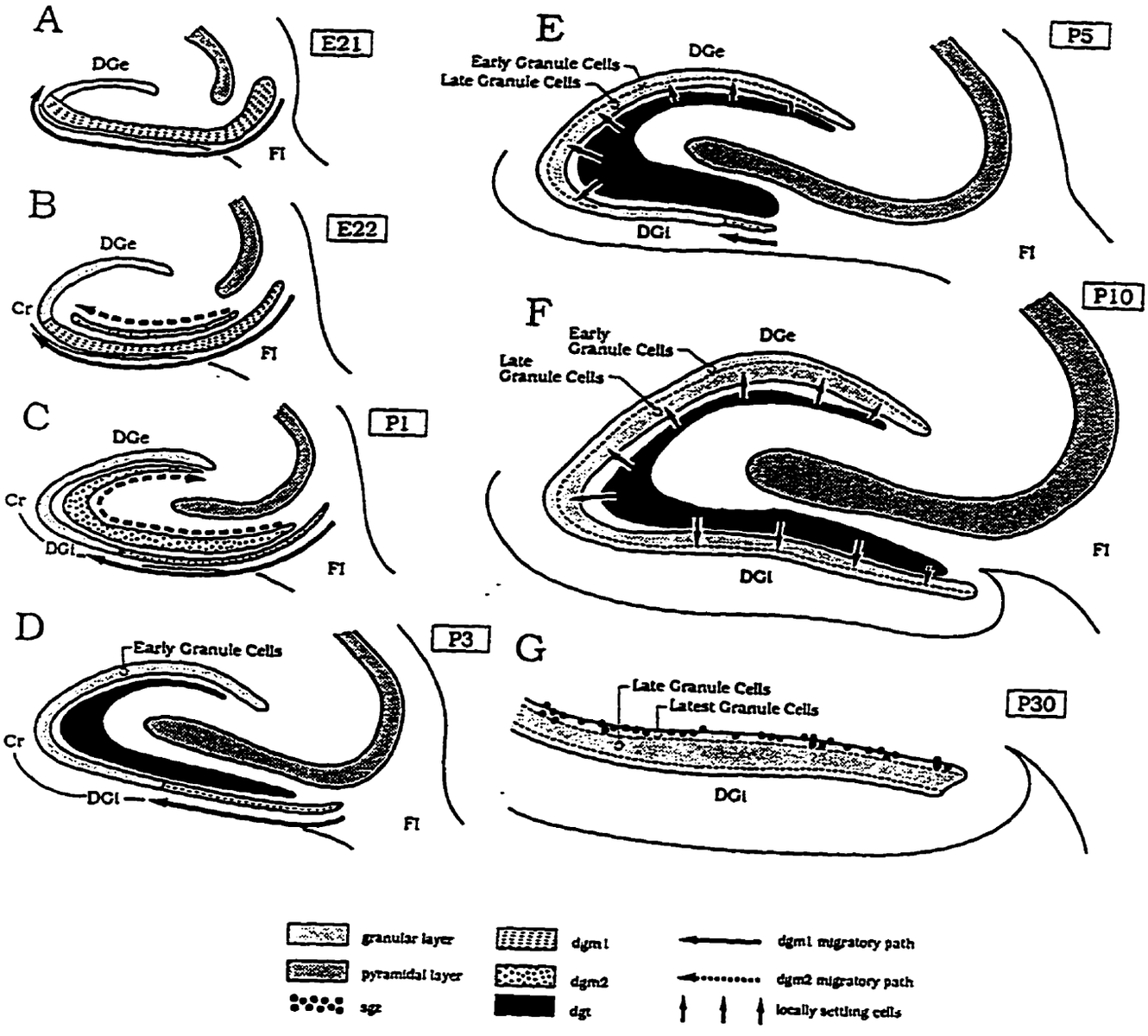
A
E21
DGe
Fl
B
E22
DGe
Cr
Fl
C
P1
DGe
Cr
DGi
Fl
D
P3
Early Granule Cells
Cr
DGi
Fl
E
P5
Early Granule Cells
Late Granule Cells
DGe
DGi
Fl
F
P10
Early
Granule Cells
Late
Granule Cells
DGe
DGi
Fl
G
P30
Late Granule Cells
Latest Granule Cells
DGi
granular layer
pyramidal layer
sgz
dgm1
dgm2
dgi
dgm1 migratory path
dgm2 migratory path
locally settling cells

neurogenesis in Ammon's horn and the dentate gyrus occurs at about the same time, granular neurons of the dentate, having originated at the same period of time continue to be produced well into post-natal life, at a time when the generation of other cell types in the hippocampus is thought to be complete (reviewed in Cowan *et al.* , 1980 and Bayer *et al.* , 1993). In animals in which neurogenesis has been studied most (mouse and rat) it is reported that no less than 80% of granular neurons are produced during the first 3 weeks after birth (Angevine, 1963; Bayer and Altman, 1974; Schlessinger *et al.*, 1975; Bayer, 1980a, 1985; Reznikov, 1991). This post-natal production of granule cells has also been observed in the rabbit (Gueneau *et al.*, 1982), cat (Altman, 1963; Wyss and Sripanidkulchai, 1985), guinea pig (Altman and Das, 1967), and rhesus monkey (Rakic and Nowakowski, 1981; Rakic, 1985; Eckenhoff and Rakic, 1988). The generation of granular neurons has further been reported to continue into adulthood in the rat (Kaplan and Hinds, 1977; Bayer, 1982; Gueneau *et al.*, 1982; Kaplan and Bell, 1984; Bayer, 1985; Crespo *et al.* , 1986; Trice and Stanfield, 1986; Stanfield and Trice, 1988; Cameron *et al.*, 1993).

During the embryonic period hippocampal development is dependent upon the migration of cells from the hippocampal neuroepithelium adjacent to the lateral ventricles (Figure 2). However, during post-natal life these ventricular germinal matrices become "exhausted", leaving the late-developing dentate gyrus dependent upon secondary extraventricular proliferative zones, namely the tertiary dentate matrix and subgranular zone (reviewed in Cowan *et al.*, 1980;

Gueneau *et al.*, 1982; Altman and Bayer, 1990a, 1990b, 1990c). These secondary proliferative zones were established through the migration (Figure 3) of putative precursor cells from the dentate neuroepithelium and serve as the source of granule cells in post-natal animals, as well as in mammals in which neurogenesis has been demonstrated to continue into adulthood (Angevine, 1963, 1964, 1965; Altman and Das, 1967; Kaplan and Hinds, 1977; Bayer, 1982; Gueneau *et al.*, 1982; Kaplan and Bell, 1984; Boss *et al.*, 1985; Stanfield and Trice 1988; Cameron *et al.*, 1993; Gage *et al.*, 1995; Kuhn *et al.*, 1996).

Unfortunately, data concerning the onset of gliogenesis in the hippocampus is lacking. Investigations of the appearance of radial glia and astrocytes report their initial detection before the onset of neurogenesis (Levitt and Rakic, 1980; Woodhams *et al.* , 1981; Eckenhoff and Rakic, 1984; Rickmann *et al.* ,1987). Furthermore, the results of several investigations illustrate that extraventricular post-natal cytogenesis within the dentate is not limited to the generation of neuronal progeny (Bayer and Altman, 1974; Schlessinger *et al.*, 1975; Bayer, 1980a; Bayer, 1985). Using combined immunohistochemical and autoradiographic techniques, Cameron *et al.* (1993) positively identified newly-generated glial cells (astrocytes) in the subgranular zone of both post-natal and adult rats. Bayer and Altman (1974) reported that the majority of the post-natally derived glial cells (about 80%) arise from the subgranular zone.

In summary, the sequence of neuro- and gliogenesis is conserved in all mammals and the post-natal production of new neurons and glia has been illustrated in numerous species. However, it has been accepted that only in the dentate gyrus of the rat, does the production of new neurons and glia continue throughout the life of the animal.

1.4 *A novel picture of mitotic activity*

In 1994 as part of a summer studentship in the in vivo laboratory of NeuroSpheres Ltd., I assisted Dr. Poulin in the development of a labeling protocol which was designed to identify slow cycling cells *in vivo*. Rationale for the experimental design was adapted from Morshead and van der Kooy (1992), who administered intraperitoneal (i.p.) injections of bromodeoxyuridine (BrdU; a thymidine analog) every two hours for a period of 12 hours, to detect the entire population of constituitively proliferating cells in the adult subventricular zone. This work established that the constituitively proliferating cells of the subventricular zone had a cell cycle time of approximately 12.7 hours, 4.2 hours of which were spent in S-phase (Morshead and van der Kooy, 1992). In addition, the existance of another population of cells characterized by small numbers, extended periods of mitotic quiescence, and cell cycles times in excess of 12 hours had been inferred by the works of Nowakowski *et al.* (1989), Craig *et al.* (1994), and Morshead *et al.* (1994). On the basis of these latter studies, Dr.

Poulin created an extended labeling protocol, adapted from Morshead *et al.* (1994), to identify these more slowly proliferating cells *in vivo*.

Although the occurrence of [^{3}H]-thymidine and/or BrdU-labeled cells in the adult mammalian hippocampus had not been reported outside the region of the dentate gyrus, preliminary data indicated that BrdU-IR cells were not restricted to previously characterized "zones of proliferation", but were instead located throughout the parenchyma. After a more detailed examination of the distribution of the labeled cells, it became apparent that the picture of mitotic activity we were observing within the hippocampus was different from what had previously been reported. That is, putative mitotically-active cells were identified in regions where proliferation was thought to be absent.

In an effort to ascertain why we were observing a different picture of mitotic activity in the region of the hippocampus, a review of the literature describing the "classic" picture of activity was undertaken. The majority of early experiments assaying mitotically-active cells in post-natal animals employed a single (i.p.) injection of [^{3}H]-thymidine given at varying concentrations (Altman, 1963; Altman and Das, 1965, 1966a; Altman, 1966). More recent studies performed in adult animals employed either the single pulse method (Kaplan and Hinds, 1977; Kaplan and Bell, 1984; Crespo *et al.* , 1986; Cameron *et al.* , 1993; Seki and Arai, 1995), or a variation of the theme by administering daily single pulses of either [^{3}H]-thymidine or BrdU over a period of 2-4 days (Bayer, 1980 a, b; Gueneau *et al.* , 1982). Both methods revealed the same picture of

mitotic activity at comparable developmental stages. If both methods revealed comparable pictures of mitotic activity in the mammalian hippocampus, why were we seeing a different one? The answer, I propose, may be due in part to potential changes in the cytokinetic conditions as an animal ages since the extended labeling protocol was designed to detect slower cycling cells.

1.5 *Cytokinetic differences in the embryonic versus adult CNS*

As an animal matures, the proportion of cells that comprise the proliferating population (i.e. growth fraction) decreases from a level of 100% in the embryo, to approximately 0.4% in an adult animal (reviewed in Korr, 1980; Schultze and Korr, 1981). Accompanying this decline is a significant increase in the average cell cycle time of proliferating cells in the population. During embryogenesis, the average cell cycle time is about 8 hours, however in the adult these times more than double to a period of approximately 20 hours (Atlas and Bond, 1965; Waechter and Jaensch, 1972; Lewis, 1978). So as an animal approaches adulthood its cellular environment, which was once characterized almost exclusively of rapidly proliferating cells, is transformed into an antithesis, where only a fraction of the cells are mitotically-active, and they take considerably longer to divide. This inverse relationship between embryonic and mature cellular environments is illustrated in Figure 4.

Considering the cytokinetic differences of the adult versus embryonic mammalian CNS, it stands to reason that standard single pulse methods (or

Figure 4. A comparison of embryonic versus adult cytokinetic conditions.

Shortly after the formation of the neural tube (E11-12), the average cell cycle time in the rodent is about 8 hours, 5 hours of which are spent in S-phase. As the animal ages cell cycle times increase, until in the mature animal the average cell cycle time is 18-20 hours, with a 7-10 hour S-phase. Accompanying this lengthening of the cell cycle is a decrease in the growth fraction. In early murine development (<E14), the growth fraction of the cells in the ventricular zone of the neural tube is 1.0, but soon after, it begins to decline sharply till reaching approximately 0.19 during juvenile life (reviewed in Korr, 1980).

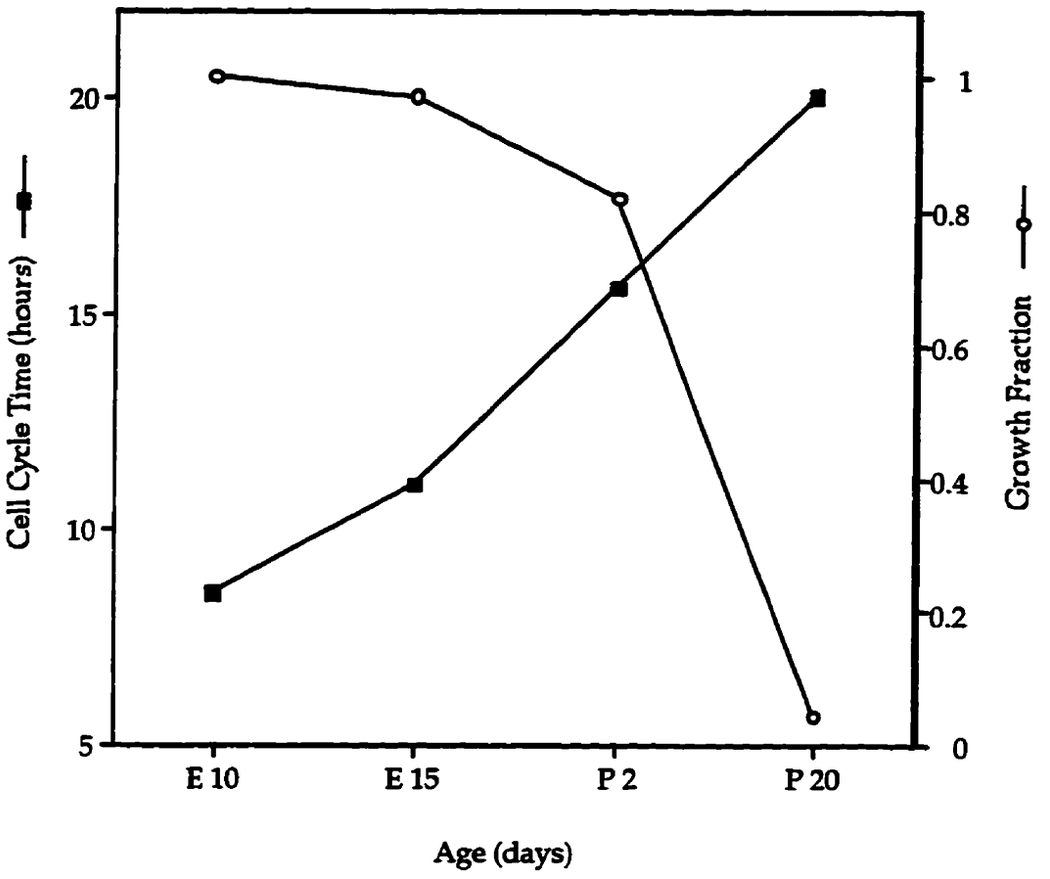
Cell Cycle Time (hours)
20
15
10
5
1
0.8
0.6
0.4
0.2
0
Growth Fraction
E 10
E 15
P 2
P 20
Age (days)

variations thereof) would reveal a much different picture of mitotic activity than protocols which attempt to account for these differences.

1.6 *Statement of Hypothesis*

A novel picture of mitotic activity within the adult mammalian hippocampus can be achieved by accounting for increased cell cycle times and decreased growth fractions in comparison to early development.

1.7 *Experimental Objectives*

(i) Develop a labeling protocol that accounts for increased cell cycle times and decreased growth fractions in the adult central nervous system.

Preliminary results demonstrated that the picture of mitotic activity we were observing was different from those that had previously been reported. This difference was attributed to the administration of the nucleotide (BrdU) every two hours for a period of 12 hours, rather than by a single pulse. This protracted window of delivery was presumed to affect the detection of proliferating cells (and the picture of mitotic activity) by exposing them to a greater amount of the nucleotide for a longer period of time. The purpose of this experiment (here after called the BrdU incorporation study) was to manipulate the concentration of BrdU, and/or the window of delivery of the nucleotide in a limited number of protocols so as to explore their relative effects

on the detection of proliferating cells. At the completion of this survey, a single protocol was selected based on the relative number and distribution of the BrdU-IR cells. This protocol was employed to investigate the identity of the BrdU-labeled cells.

(ii) Establish that the chosen protocol does not produce a toxic effect on the BrdU-labeled cells.

Before we can begin an investigation into the fate of the BrdU-IR cells it is important to determine whether the labeling protocol chosen, in fulfillment of the first experimental objective, will cause toxic side effects in the labeled cells. It has been demonstrated that when high levels of nucleotides such as BrdU are incorporated into proliferating cells, cytotoxic effects such as an inhibition in the cell cycle may result (reviewed below). To assay for any potential toxic effects, a second set of animals were adminstered the same frequency of injections using [^{3}H]-thymidine. It is important to employ a dose of [^{3}H]-thymidine which has previously been demonstrated not to produce any detectable toxic effects. Following the completion of the [^{3}H]-thymidine and BrdU injection protocols, a comparison of the number and distribution of labeled cells using each method should elucidate any cytotoxic changes.

(iii) Establish the fate of the BrdU labeled cells at various periods following the incorporation of the nucleotide.

The purpose of this experiment was to investigate what happens to the BrdU-IR cells over time as a function of number, distribution and fate. This was accomplished by perfusing the animals immediately following the completion of the BrdU injection protocol, and at survival times of 3, 6, 9, 12, and 24 weeks. By employing double-label immunocytochemistry using known markers for neurons (NeuN, Calbindin) and astrocytes (GFAP, S-100) at these time points we can establish which phenotypes are produced and their temporal appearance in the hippocampus.

2. MATERIALS AND METHODS

Adult male CD-1 mice (29-33 grams) were obtained from Charles River and kept on a standard laboratory diet with free access to water and food. Following the injection of either BrdU or [^{3}H]-thymidine (see below), animals were deeply anesthetized with sodium pentobarbital (intraperitoneal injection of Nembutal, 0.1 mL) and perfused transcardially first with 0.9% saline (NaCl) followed by a fixative solution (4.0% paraformaldehyde in 0.1 M phosphate buffer, pH 7.4). The brain was removed from the skull and postfixed overnight at 4°C in the same fixative solution. Following post fixation, brains were cryoprotected in 10% then 20% sucrose (in 0.1M phosphate buffered saline) overnight at 4°C, followed by a solution of 20% sucrose (in 0.1M PBS) with Tissue-Tek OCT embedding compound at a ratio of 2:1 overnight. Brains were embedded in OCT and frontal sections were cut with a MICROM cryostat. All sections were cut at 14µm except for those in the BrdU incorporation study, which were cut at 30µm. Serial sections were mounted on gelatin coated slides and dried at room temperature. Slides were stored at -80°C until needed. Immediately before processing the slides were removed from the freezer, allowed to warm to room temperature, and air dried.

2.1 *Labeling of mitotically-active cells*

2.1.1 *BrdU incorporation study labeling protocol*

The region of the dentate gyrus was arbitrarily chosen as a representative structure through which to examine the effects of various labeling protocols. Animals were administered (i.p.) injections every two hours with 0.15 mL of BrdU (Sigma, dissolved in 0.007N NaOH in 0.9% NaCl) at concentrations of 1.8, 9.0, and 18.0 mg/mL for a period of 12, 24, 48, and 72 hours (see Figure 5). The 12, 24, and 48 hour labeling protocols were preceded with the administration of physiological saline, in order to assure that all animals received an equal number of injections. Control mice received 0.15 mL injections of physiological saline for the duration of the injection protocol. In all cases, 30 minutes after the last injection was administered, the animals were perfused and their brains sectioned and processed for BrdU immunocytochemistry (Granzber, 1982).

2.1.2 *BrdU-[^{3}H]-thymidine toxicity study labeling protocol*

Two sets of animals received i.p. injections of either 0.15 mL of BrdU (9.0 mg/mL dissolved in 0.007N NaOH in 0.9% NaCl; 45 mg/kg body weight) or 0.10 mL of [^{3}H]-thymidine (6.7 Ci/mmol; 8.33 µCi/injection; ICN Biomedical; 10 mg/kg B.W.) every two hours for 48 hours. At the completion of the injections, each animal had received a total of either 32.4 mg of BrdU (1080 mg/kg B.W.) or 7.21 mg of [^{3}H]-thymidine (240 mg/kg B.W.). All control mice

Figure 5. A schematic representation of BrdU injection protocols.

All animals were administered one injection (i.p.) every two hours for a period of 72 hours. Bold lines indicate the time course of BrdU injections, while thin lines indicate the time course of saline injections. The 12, 24, and 48 hour BrdU injection protocols were preceded with the administration of physiological saline to assure that all animals received an equal number of injections. Three concentrations of BrdU (1.8, 9.0, and 18.0 mg/mL) were employed for each time period (i.e. 24 hours), with four animals (n = 4) in each condition.

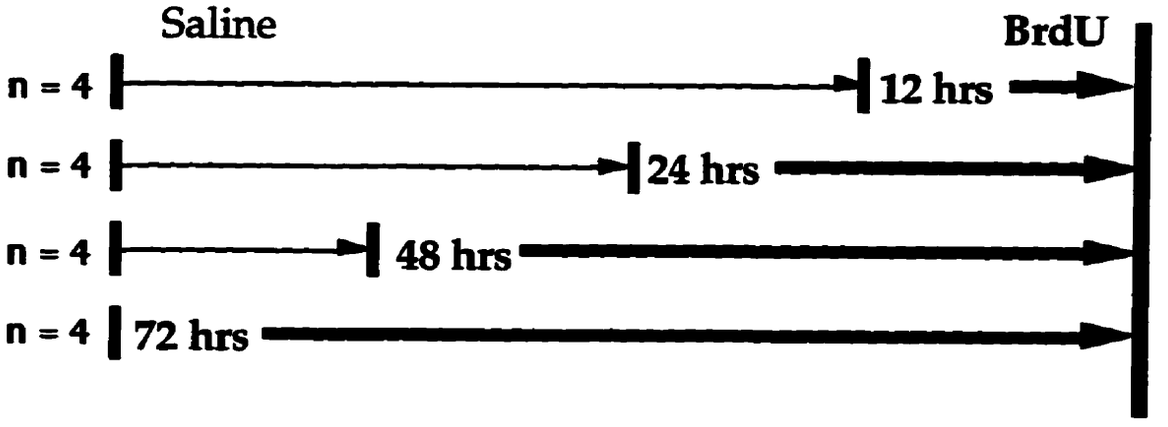
Saline
BrdU
n = 4
12 hrs
n = 4
24 hrs
n = 4
48 hrs
n = 4
72 hrs

received 24 injections of 0.15 mL physiological saline. 30 minutes following the last injection, all animals were sacrificed and their brains removed, sectioned, and processed for either BrdU immunocytochemistry or [^{3}H]-thymidine autoradiography. The BrdU-[^{3}H]-thymidine parallel labeling experiment was performed on three separate occasions, with each trial employing three animals in either condition.

Rationale for the [^{3}H]-thymidine labeling protocol used in this study came from Lois and Alvarez-Buylla (1993), who labeled dividing cells with the same protocol, except only for 12 hours. In their study Lois and Alvarez-Buylla (1993) demonstrated that the cells which were labeled *in vivo*, differentiated directly into neurons and glia *in vitro*. In further studies, Lois and Alvarez-Buylla (1994) injected 10 nanoliters of [^{3}H]-thymidine (1 mCi/mL; specific activity = 6.7 Ci/mmol) directly into the lateral ventricles of an adult mouse assaying for the same cells. The labeled cells migrated from the ventricles towards the olfactory bulb at a rate of 30 μm per hour (similar to that reported for tangentially migrating young neurons during development (O'Rourke *et al.*, 1992; Fishell *et al.*, 1993)), proliferating enroute and differentiating into neurons upon reaching their destination. This investigation further suggests that the incorporation of an even higher dose of the nucleotide, failed to produce an inhibition in proliferation or other cytotoxic effect (Spector, 1980; Spector and Berlinger, 1982). Olsson (1976) demonstrated that a single i.p. injection of [^{3}H]-thymidine (1.0 μCi/g B.W.; specific activity 5.0 Ci/mmol) into an adult mouse would

induce only a temporary inhibition in the cell cycle of proliferating epidermal cells.

In comparison to the above cited works, the dose of [^{3}H]-thymidine employed in the BrdU-[^{3}H]-thymidine toxicity study has: (a) a lower concentration (0.25μCi/g B.W. versus 1.0μCi/g B.W.) than that needed to induce even a temporary inhibition in the cycle of cells outside the blood brain barrier, (b) a lower concentration (83.3 μCi/mL versus 1.0 mCi/mL) than Lois and Alvarez-Buylla (1994), who injected [^{3}H]-thymidine directly into the lateral ventricles and observed no apparent cytotoxic effects, and (c) an identical concentration and specific activity to that of Lois *et al.* (1993). The studies cited above indicate that the [^{3}H]-thymidine labeling protocol employed in this work does not cause cytotoxic stress on the labeled cells.

2.1.3 *Fate of BrdU-immunoreactive cells over time.*

Eighteen mice were administered injections of BrdU (45 mg/kg B.W. per injection) every two hours for a period of 48 hours (1080 mg/kg B.W. in total). Thirty minutes following the last injection (considered day zero) 3 animals were perfused and their brains removed. The remaining mice were perfused and their brains removed at survival times of 3, 6, 9, 12, and 24 weeks (n=3 for each). After sectioning each brain (14μm), double label immunocytochemistry was performed on BrdU-immunoreactive (BrdU-IR) cells using known markers for

neurons (NeuN and Calbindin) and astrocytes (GFAP). Previous studies have shown that in the brain: (i) NeuN recognizes a neuronal specific nuclear protein (Mullen *et al.*, 1992), (ii) GFAP is expressed exclusively by glia (Kalman and Hajos, 1989; Hajos and Kalman, 1989), (iii) S-100 is also exclusively expressed in astrocytes (Matus and Mughal, 1975; Ghandour *et al.*, 1981a), and (iv) Calbindin D28-k is present in all dentate granule cells, and some, but not all, CA1 and CA2 pyramidal cells (Sloviter, 1989; Celio, 1990).

2.2 *Immunocytochemistry*

2.2.1 *BrdU immunocytochemistry*

Sections processed for BrdU were rinsed in washing solution (0.1 M PBS containing 0.02% sodium azide) for 20 minutes before any immunocytochemistry was performed. The sections were incubated in 1.0N HCl for 30 minutes at 60°C to denature the DNA, then rinsed in washing solution (3 X 15 minutes), and incubated overnight at room temperature in a primary rat monoclonal antibody (1:50) directed against single-stranded DNA containing BrdU (Seralab). The next morning, the sections were rinsed in washing solution (3 X 15 minutes) and incubated for 1 hour in anti-rat IgG FITC (Jackson, diluted 1:100 in washing solution) at room temperature then rinsed and coverslipped under FluorSave (Calbiochem). Staining controls for this section involved the deletion of the anti-mouse BrdU antibody from the labeling

protocol. Each negative control was processed alongside a positive control for validity.

2.2.2 *Double labeling immunocytochemistry*

Sections processed were rinsed in washing solution (0.1 M PBS containing 0.02% sodium azide) for 20 minutes before any immunocytochemistry was performed. The sections were then incubated overnight at room temperature (RT) in a solution containing mouse monoclonal antibodies to either GFAP (Boehringer Mannheim, 1:200), S-100 (Sigma, 1:500), or NeuN (gift from Dr. R. Mullen, 1:50) all diluted in 0.1M PBS + 0.3% triton + 10% normal goat serum. The sections were then rinsed in washing solution (3 X 15 minutes) and incubated in anti-mouse IgG CY3 (Jackson, diluted 1:100 in washing solution) for 1 hour (RT). Sections processed for Calbindin immunoreactivity were incubated for 3 days at 4°C in a solution containing rabbit polyclonal antisera to Calbindin D28K (gift from Dr. K. Baimbridge, 1:500) diluted in 0.1M PBS + 0.3% triton + 20% normal goat serum + 1.0 mMol EDTA + 20 units/mL heparin. The sections were then rinsed in washing solution (3 X 15 minutes), incubated for 1 hour (RT) in biotin-conjugated anti-rabbit IgG (Jackson, diluted 1:500 in washing solution), rinsed again (3 X 15 minutes), and incubated for 1 hour (RT) in streptavidin conjugated CY3 (Jackson, diluted 1:1000 in washing solution). Following the completion of the first label, the sections were rinsed again in washing solution (3 X 15 minutes), then incubated in 1.0N HCl for 30 minutes at

60°C to denature the DNA. Following incubation, sections were rinsed in washing solution (3 X 15 minutes), and incubated overnight at room temperature in a primary rat monoclonal antibody (1:50) directed against single-stranded DNA containing BrdU (Seralab). Finally, the sections were rinsed in washing solution (3 X 15 minutes), and incubated for 1 hour in anti-rat IgG FITC (Jackson, diluted 1:100 in washing solution) at room temperature, then rinsed in washing solution (3 X 15 minutes) and the slides were coverslipped under FluorSave (Calbiochem). Controls for each of the two phases of the double label were performed by the deletion of the respective primary antibody. Alongside each negative control, a positive control was processed for validity. In the case of calbindin immunoreactivity, two sources of anti-calbindin were employed (Calbindin D-28k; gift from Dr. K. Baimbridge and Anti-Calbindin-D; Sigma). In both cases, an identical pattern of labeling was observed.

2.3 *Autoradiography*

Those slides prepared for autoradiography were dipped in Kodak NTB-3 (diluted 1:1 in ddH_2O) emulsion and exposed for 14 days at 4°C. Slides were then developed in Dektol (Kodak), rinsed in ddH_2O, fixed in Ektaflo (Kodak), rinsed again, stained for Nissl using Cresyl Violet and coverslipped under Permount. Control sections were processed as described above.

2.4 *Cell counts and quantification*

All slides were coded prior to microscopic analysis and the code was not broken until the analysis was complete. Three sections were examined at each rostral (-1.3), mid (-2.1), and caudal (-2.9) coordinate as measured from bregma (Sidman *et al.*, 1971), to assure consistency in counts between animals. At each coordinate, all the regions of Ammon's horn and both blades of the dentate gyrus were visible. Demarcation of the boundaries employed to distinguish CA1, CA2-3 and dentate gyrus regions of the hippocampus are illustrated by solid lines in Figure 1. The counting area of the dentate gyrus was further distinguished by the hippocampal fissure and hippocampal sulcus, as was Ammon's horn by the lateral ventricles. Cell counts for the number of BrdU-IR cells in each study were corrected as previously described in Ambercrombie (1946). Cells were considered BrdU-IR by examining their morphologies, patterns of fluorescence, and intensity of fluorescence. Any cell which exhibited an autofluorescent signal, or had an uncharacteristic morphology were not counted.

2.5 Image Analysis

Photomicrographs were created by first capturing the image using Kodak Ektachrome Elite 400 slide film. Processed slides were then digitized, cropped, and corrected for brightness and contrast using Adobe Photoshop 3.0 for Macintosh.

3.0 RESULTS

3.1 *BrdU incorporation study*

To study the effect of manipulating the concentration and time course of delivery of BrdU on the detection of mitotically-active cells, animals were administered BrdU at concentrations of 1.8, 9.0, and 18.0 mg/mL every two hours for 12, 24, 48, and 72 hours (Figure 5). Under all conditions examined, BrdU-IR cells were detected not only in the region of the dentate gyrus, but also throughout Ammon's horn (Figure 6). The highest density of immunoreactive cells were found in the region of the subgranular zone directly below the granule cell layer of the dentate gyrus (Figure 6). Doublets of BrdU-IR cells (arrows, Figure 6) were evident throughout the hippocampus, with their highest incidence in the subgranular zone.

The region of the dentate gyrus was arbitrarily chosen as a representative structure through which to examine the relative effects of the manipulating the concentration of nucleotide and period of injections. Quantitative analysis revealed that regardless of the concentration of BrdU employed, the 12 hour protocol did not detect the greatest number of BrdU-IR cells in comparison to longer time periods (Figure 7). Focusing on the 9.0 mg/mL data points, a leveling off in cell number is evident between the 48 and 72 hours. This "plateau" was not realized when a lower concentration (1.8 mg/mL) of BrdU

Figure 6. Distribution of BrdU-immunoreactive cells in the hippocampus.

Photomicrographs of BrdU-IR cells in a caudal section of the hippocampus demonstrating the presence of labeled cells in various regions of the dentate gyrus and Ammon's horn. The highest concentration of BrdU-IR cells was observed in the subgranular zone. Note the presence of doublets (arrows) throughout. Scale bar = 88μm.

Figure 7. Quantitative analysis of BrdU-immunoreactive cells in the dentate gyrus.

In order to assure that homologous regions of the dentate were counted throughout the experiment, 3 individual (30μm) tissue sections were quantified at each rostral, medial, and caudal coordinate. Then the mean number of BrdU-IR cells for each coordinate was calculated, providing a rostral, medial, and caudal mean cell count. Finally, the mean cell counts derived from the rostral, medial, and caudal coordinates were added together, to provide a representative total number of cells for each animal. Figure 7 illustrates this representative total cell count for each condition as a function of labeling period. Error bars represent the standard deviation from the mean for averages within each condition for one set of experiments.

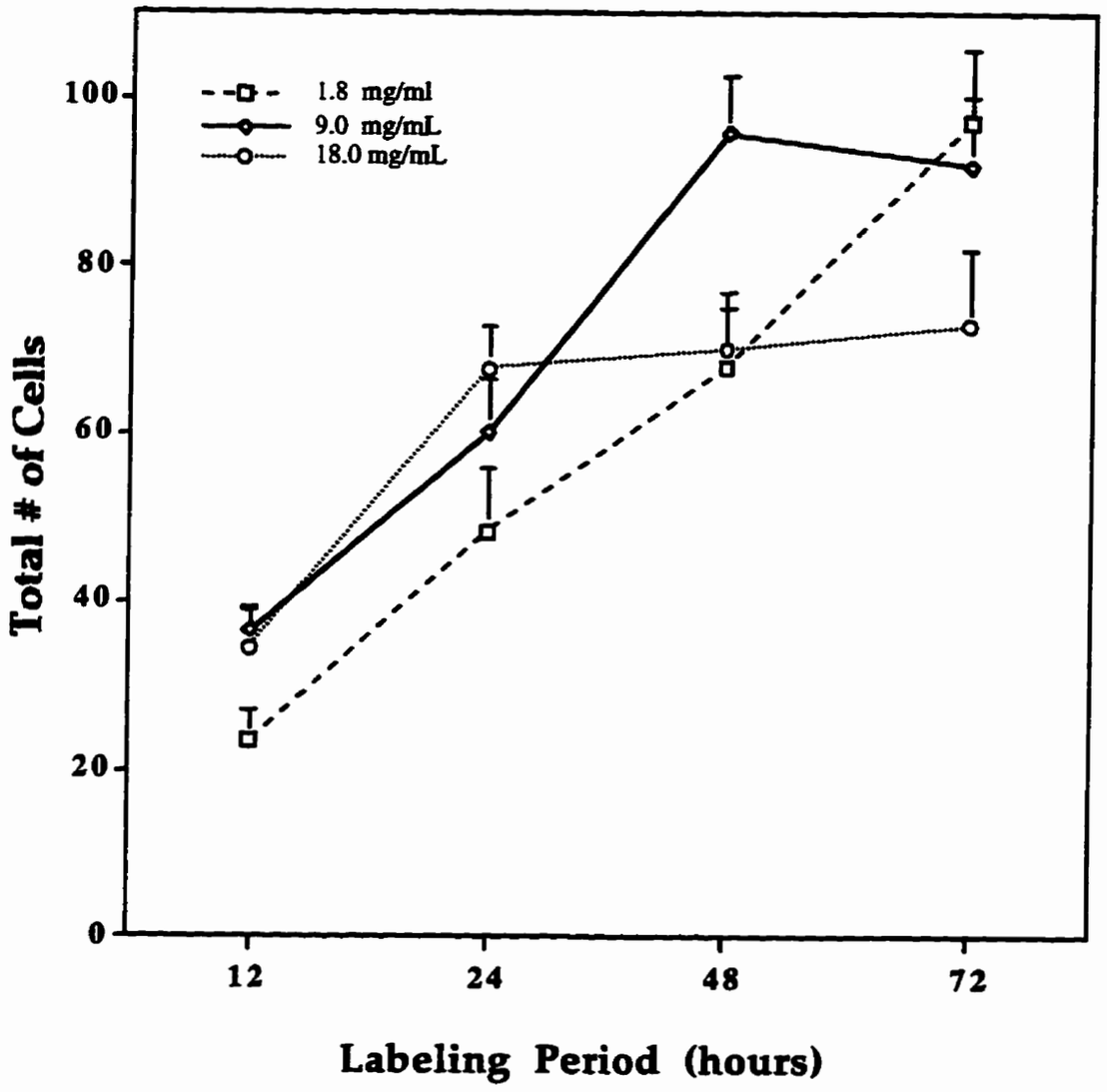
1.8 mg/ml
9.0 mg/mL
18.0 mg/mL
100
80
60
40
20
0
Total # of Cells
12
24
48
72
Labeling Period (hours)

was employed, but is apparent at an earlier time point (24 hrs.) when higher concentrations (18.0 mg/mL) of BrdU were employed. The detection of the greatest amounts of BrdU-IR cells for this set of experiments was achieved by employing concentrations of 1.8 mg/mL over 72 hours (97 ± 9 cells), or 9.0 mg/mL over 48 hours (96 ± 8 cells). Though both protocols detected an equivalent number of cells, the latter was selected to investigate the identity of the BrdU-IR cells and ascertain the potential toxic effects of incorporating the BrdU nucleotide.

3.2 *BrdU-[^{3}H]-thymidine toxicity study*

As outlined in the methods section (2.1.2), three animals in three separate trials received either: (a) 0.10 mL i.p. injections of 10 mg/kg B.W. of [^{3}H]-thymidine (8.33 μCi/injection; specific activity = 6.7 Ci/mmol), or (b) 0.15 mL i.p. injections of 45 mg/kg B.W. of BrdU, every two hours for 48 hours. Upon completion of the injection protocols, cells which had incorporated the respective nucleotides were observed both in the dentate gyrus and Ammon's horn regions in every brain examined. Quantitative analysis revealed that in all three regions of the hippocampus (i.e. CA1, CA2-3, dentate gyrus), [^{3}H]-thymidine had consistently tagged fewer cells (approx. 27%) than BrdU (Figure 8). An analysis of variance confirmed that when rostral, medial, and caudal cell counts were combined, significantly fewer cells ($F=82.66$, $p<0.01$; Tukey HSD

Figure 8. [^{3}H]-thymidine detected significantly fewer cells than BrdU within each hippocampal region.

In each animal, three individual tissue sections (14μm) were quantified at rostral, medial, and caudal coordinates through the length of the hippocampus. The mean number of detected cells for each coordinate was calculated, providing a rostral, medial, and caudal mean cell count. An analysis of variance demonstrates that when rostral, medial, and caudal mean cell counts are combined, [^{3}H]-thymidine consistently detected significantly fewer cells than BrdU in each of the three regions (i.e. dentate gyrus, CA1, CA2-3) of the hippocampus counted ($F=82.66$, $p<0.01$; Tukey HSD test). Error bars represent the standard deviation from the mean within each condition in three experiments.

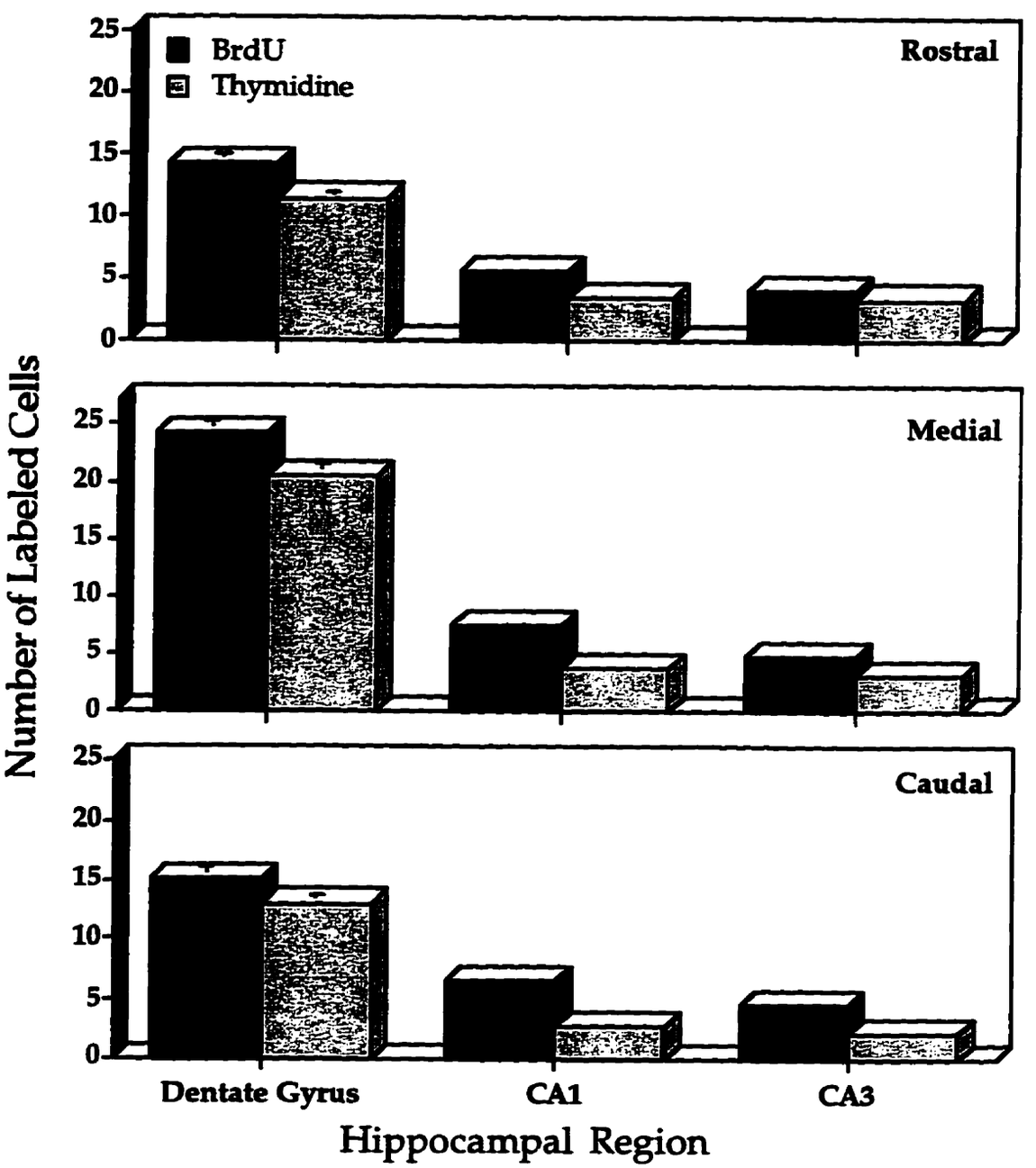
BrdU
Thymidine
Rostral
Medial
Caudal
25
20
15
10
5
0
Number of Labeled Cells
Dentate Gyrus
CA1
CA3
Hippocampal Region

test) were detected in the regions of the dentate gyrus, CA1, and CA2-3 by [^{3}H]-thymidine than BrdU.

The distribution of [^{3}H]-thymidine-labeled cells throughout the dentate gyrus (Figures 9 and 10) all the subfields of Ammon's horn (Figure 11), mimicked that of previously described BrdU-IR cells. The highest density of [^{3}H]-thymidine-labeled cells occurred in the subgranular zone of the dentate (Figure 9). Doublets of [^{3}H]-thymidine labeled cells were evident throughout the hippocampus, but were observed preferentially in stratum radiatum and stratum lacunosum moleculare of Ammon's horn (Figure 11A), as well as the hilar region of the dentate gyrus (Figure 10). The occasional occurrence of clusters of three or more [^{3}H]-thymidine labeled cells was only observed in the crest region (Figure 9D) and subgranular zone of the dentate gyrus.

In summary, [^{3}H]-thymidine detected significantly less cells in comparison to BrdU, but the distribution of cells detected with both methods was virtually identical, as was the occurance of mitotic doublets. These results are consistent with the premise that the BrdU labeling protocol does not cause any discernable toxic effects in proliferating cells.

3.3 *Fate of BrdU-immunoreactive cells over time.*

In order to determine what cell types (if any) were being produced in the hippocampus over time, double label immunocytochemistry was performed

Figure 9. [^{3}H]-thymidine labeled cells are present in the granule cell layer of the dentate gyrus.

Cresyl violet stained autoradiograms of [^{3}H]-thymidine labeled cells in the superficial aspect of the suprapyramidal limb (B), crest region (D), and deep portions of the granule cell layer in the infrapyramidal limb(C) of the dentate gyrus. A representation of the fields of view (b-d) is provided in (A). Scale bar in D (10 μm) applies to B and C as well.

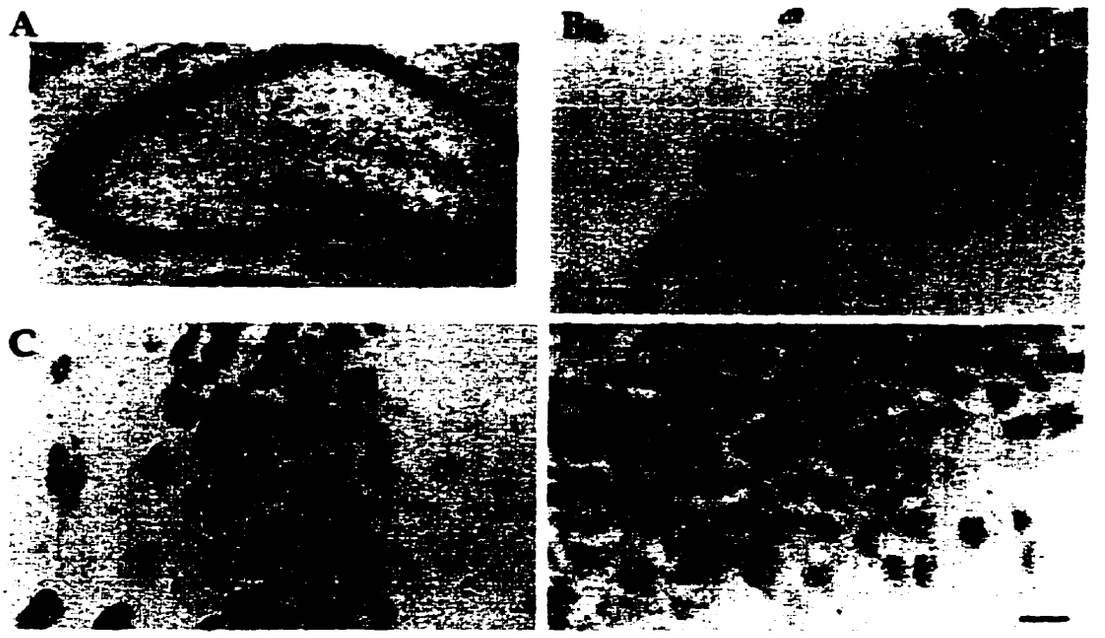
A
B
C

Figure 10. [^{3}H]-thymidine labeled cells are present in the hilar region of the dentate gyrus.

Cresyl violet stained autoradiograms of [^{3}H]-thymidine labeled cells within the hilus close to the crest (B), infrapyramidal (C) and suprapyramidal (D) regions of the dentate gyrus. Note the appearance of a possible mitotic doublet in (C) adjacent to the granule cell layer. A representation of the fields of view (b-d) is provided in (A). Scale bar in D (10μm) refers to B and C as well.

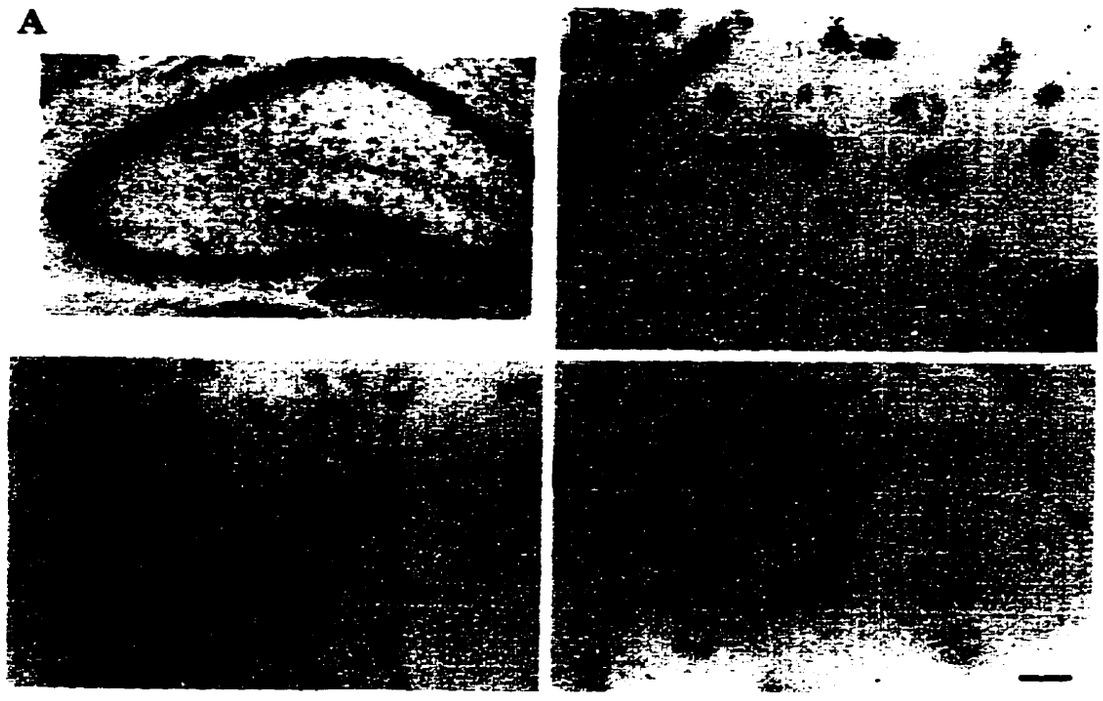
A

Figure 11. [^{3}H]-thymidine labeled cells are present in Ammon's horn.

Cresyl violet stained autoradiograms of [^{3}H]-thymidine-IR cells within stratum radiatum of CA2 (A), and immediately adjacent to the CA1 pyramidal cell layer. The two labeled cells in close approximation in (A) suggest a possible mitotic doublet. Note the difference in size of cresyl violet stained [^{3}H]-thymidine labeled cells versus cresyl violet stained unlabeled cells. Scale bar in B (10μm) refers to both panels.

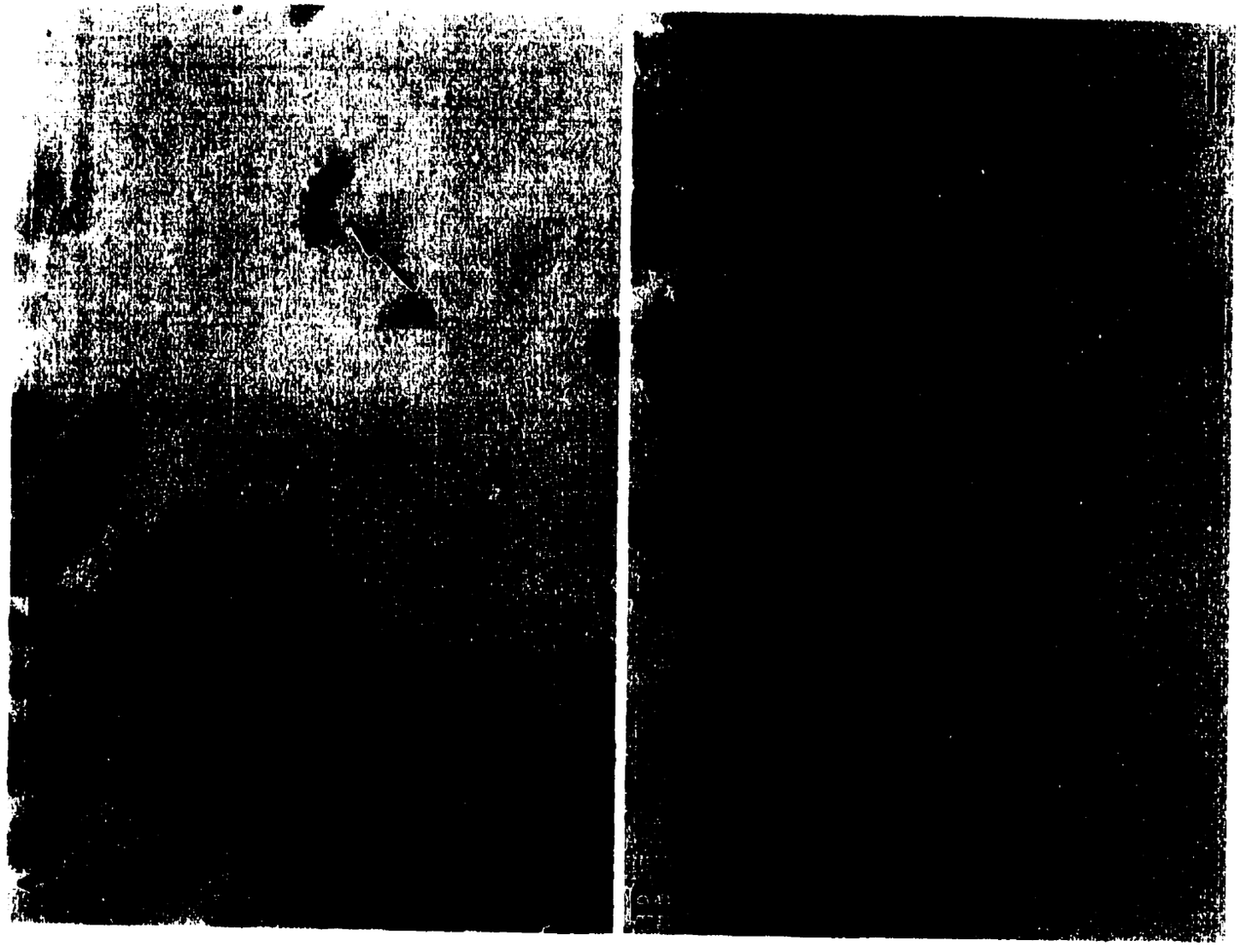

on BrdU-IR cells using known markers (see Methods section 2.2.2) for neurons (NeuN, Calbindin) and astrocytes (GFAP, S-100) at d0 , 3, 6, 9, 12, and 24 weeks (n=3 for each), following the completion of the 48 hour BrdU injection protocol.

3.3.1 *Location and number of BrdU-immunoreactive cells.*

At all time points examined, BrdU-IR cells were observed throughout the dentate gyrus and in all regions of Ammon's horn. Once again, the greatest density of BrdU-IR cells was in the subgranular zone of the dentate gyrus (data not shown). The presence of doublets within the hippocampus became restricted to the deep aspects of the granule cell layer as well as stratum radiatum and stratum oriens of Ammon's horn as survival times increased. At the latest survival time examined (24 weeks), only one doublet per brain was observed. In contrast to day zero, BrdU-IR cells did not remain uniform in size or intensity of signal as survival times increased (discussed below).

Figure 12 represents the quantitative analysis of the average number of BrdU-IR cells as a function of survival time. The greatest number of BrdU-IR cells were detected at day zero, when approximately (20 ± 4) and (18 ± 5) cells were observed in the dentate gyrus and Ammon's horn respectively

Figure 12. The number of BrdU-immunoreactive cells falls significantly over time.

Three individual tissue sections were quantified at each rostral, medial, and caudal coordinate. Then the mean number of BrdU-IR cells for each coordinate was calculated providing a rostral, medial, and caudal mean cell count. Finally, average of the mean cell counts was derived, providing a representative average number of BrdU-IR cells for any section within the hippocampus. For comparison purposes cell counts were divided into dentate gyrus, CA1 and CA2-3 regions. Within each of the three regions, a significant decline in the number of cells detected at day zero versus 24 weeks occurs ($p<0.01$; two tailed T-test). Error bars represent the standard deviation from the mean for averages within each time point for three animals in one experiment.

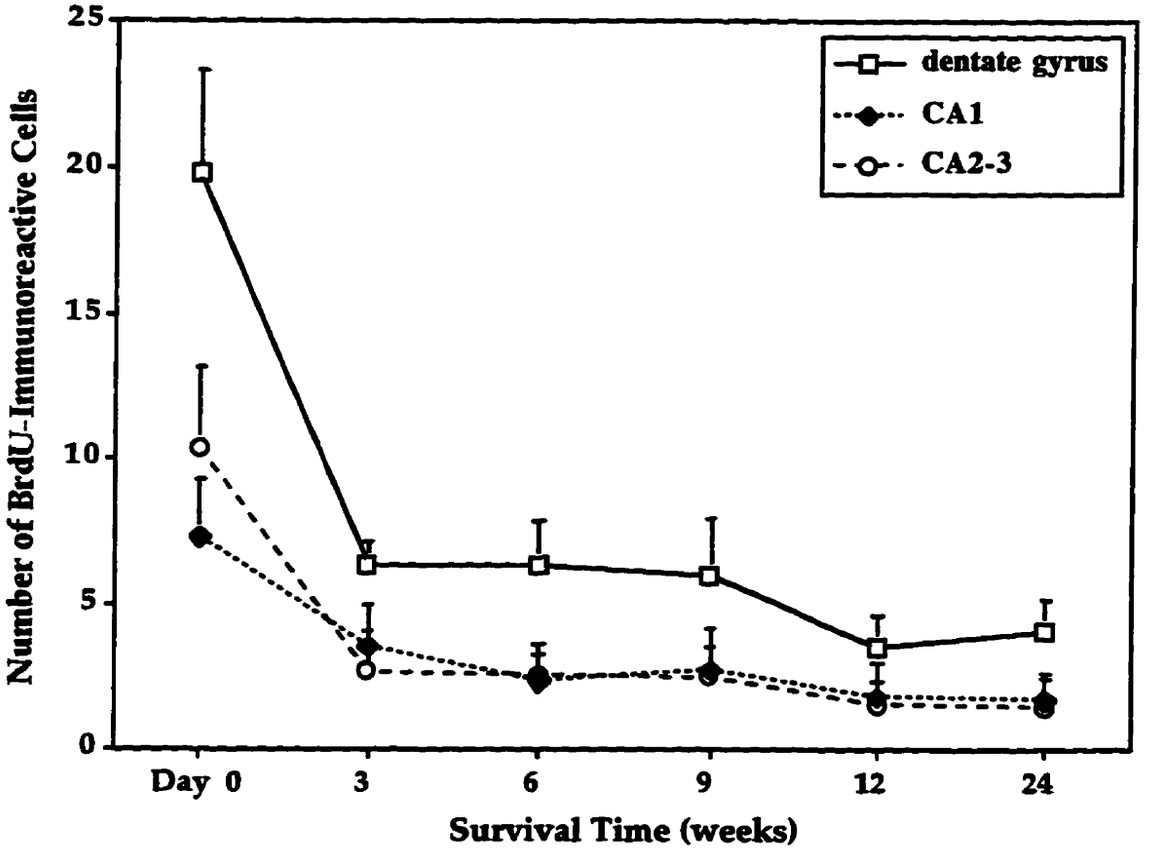
25
20
15
10
5
0
Number of BrdU-Immunoreactive Cells
dentate gyrus
CA1
CA2-3
Day 0
3
6
9
12
24
Survival Time (weeks)

(Figure 12). These counts translate into approximately 1% of the total cell number in each region being BrdU-IR. By 24 weeks, a significant reduction in the number of BrdU-IR cells had occurred, with approximately 4 ± 1 cells (0.18%) in the dentate and 2 ± 1 cells (0.20%) in Ammon's horn being detected (in both cases $p<0.01$; two tailed T-test) (Figure 12). Although a dramatic decrease in the overall number of BrdU-IR cells was realized over 24 weeks, the patterns of decline between the two regions of Ammon's horn and the dentate gyrus remained relatively consistent. The relationship between the density of BrdU-IR cells in CA1 versus CA2-3 also remained virtually unchanged throughout the time course of study.

3.3.2 *BrdU-immunoreactive cells differentiate into neurons and glia in the dentate gyrus.*

Thirty minutes following the completion of the labeling protocol (d0), none of the BrdU-IR cells examined in the dentate gyrus appeared double-labeled for either neuronal (NeuN) or glial (GFAP, S-100) markers (Figure 13). However, at the next time point examined (3 weeks) over half (~58.6%) of the BrdU-IR cells were NeuN-IR, while a smaller portion (~13%) were GFAP-IR. As survival times increased, the number of BrdU-GFAP double-labeled cells remained relatively unchanged, while the percentage of BrdU-NeuN-IR cells declined significantly to approximately 20.2 % at 24 weeks ($p<0.01$; two tailed T-test) (Figure 13).

Figure 13. Over time BrdU-immunoreactive cells express neuronal and glial antigens in the region of the dentate gyrus.

Percentage of BrdU-IR cells in the dentate gyrus which were NeuN-IR (solid bar) and GFAP-IR (stippled bar) at different survival times following the administration of BrdU. A comparison of the number of double-labeled cells at 3 weeks and 24 weeks reveals no significant difference in the percentage of BrdU-GFAP-IR cells, but a significant decrease in the percentage of BrdU-NeuN-IR cells ($p<0.01$; two tailed T-test). Error bars represent mean + S.D.

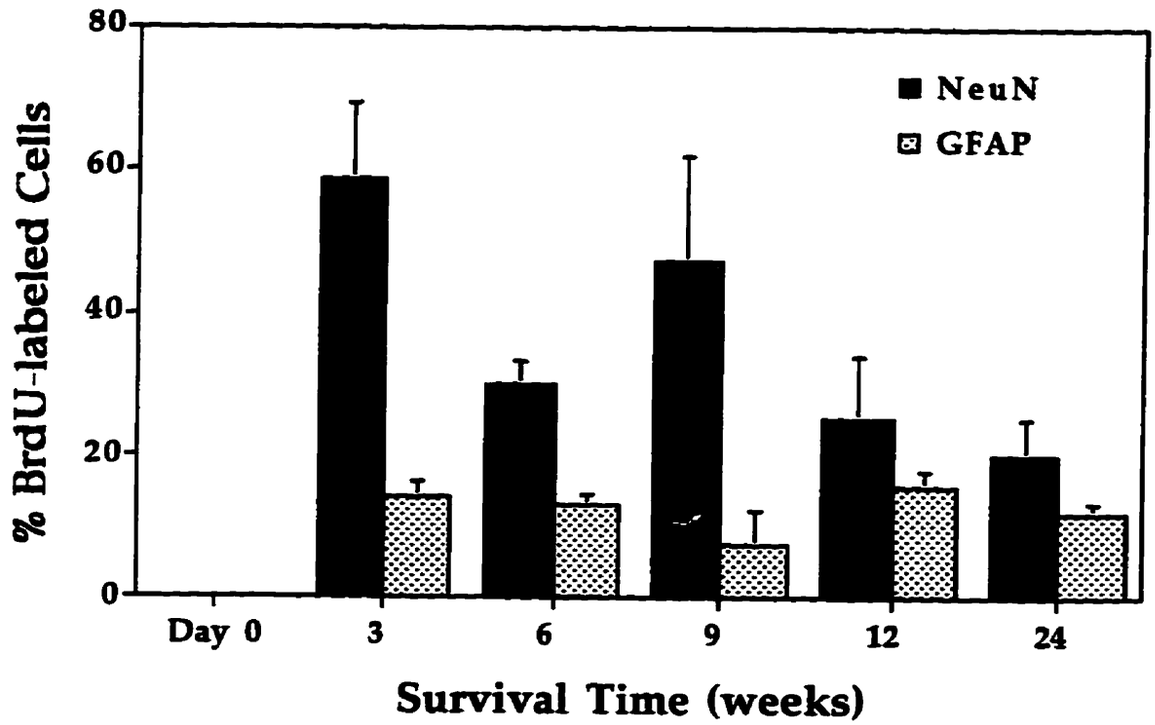
80
60
40
20
0
% BrdU-labeled Cells
NeuN
GFAP
Day 0
3
6
9
12
24
Survival Time (weeks)

Although the vast majority of BrdU-GFAP-IR cells in the dentate were located outside the granule cell layer (Figure 14B), examples of BrdU-GFAP-IR cells were occasionally observed within the granule cell layer (Figure 14A). For the most part, BrdU-GFAP-IR cells within the hilus and molecular layers displayed morphologies (small cell bodies and numerous stellate processes extending into the granule cell layer) characteristic of mature astrocytes (Figure 14A).

In contrast to the labeling pattern described above, the majority of BrdU-NeuN-IR cells were located within the granule cell layer. This made the confirmation of BrdU-NeuN-IR cells somewhat difficult to discern due to the overlapping of neuronal cell bodies. However, examples of BrdU-NeuN-IR cells were detected immediately adjacent to the subgranular zone as well as in the hilar region, making the confirmation of the double-label coincident more certain (Figure 15A,B). To assure that the double-label coincident was genuine, a second neuronal marker, Calbindin, was employed (Figure 15 C-H). The distribution of BrdU-Calbindin- and BrdU-NeuN-IR cells were virtually identical, with the majority of the BrdU-Calbindin-IR cells being located in the granule cell layer.

Figure 15 illustrates both BrdU-NeuN- and BrdU-Calbindin-IR cells in the dentate gyrus. Generally, the BrdU-IR nuclei of NeuN-IR cells (long arrow, Figure 15A) were considerably larger than those which did not exhibit NeuN-immunoreactivity (short arrow, Figure 15A). Further, as BrdU-IR nuclei became

Figure 14. Examples of BrdU-S-100- and BrdU-GFAP-immunoreactive cells in the dentate gyrus.

Photomicrographs of BrdU-IR cells (processed at 6 weeks) that are GFAP-immunoreactive (A, arrows) and S-100-immunoreactive (B) in the dentate gyrus. Note the mature stellate morphology of double-labeled cells both within the granule cell layer and within the subgranular zone in A (arrows). Scale bar in A = 20 μm, while bar in B = 10μm.

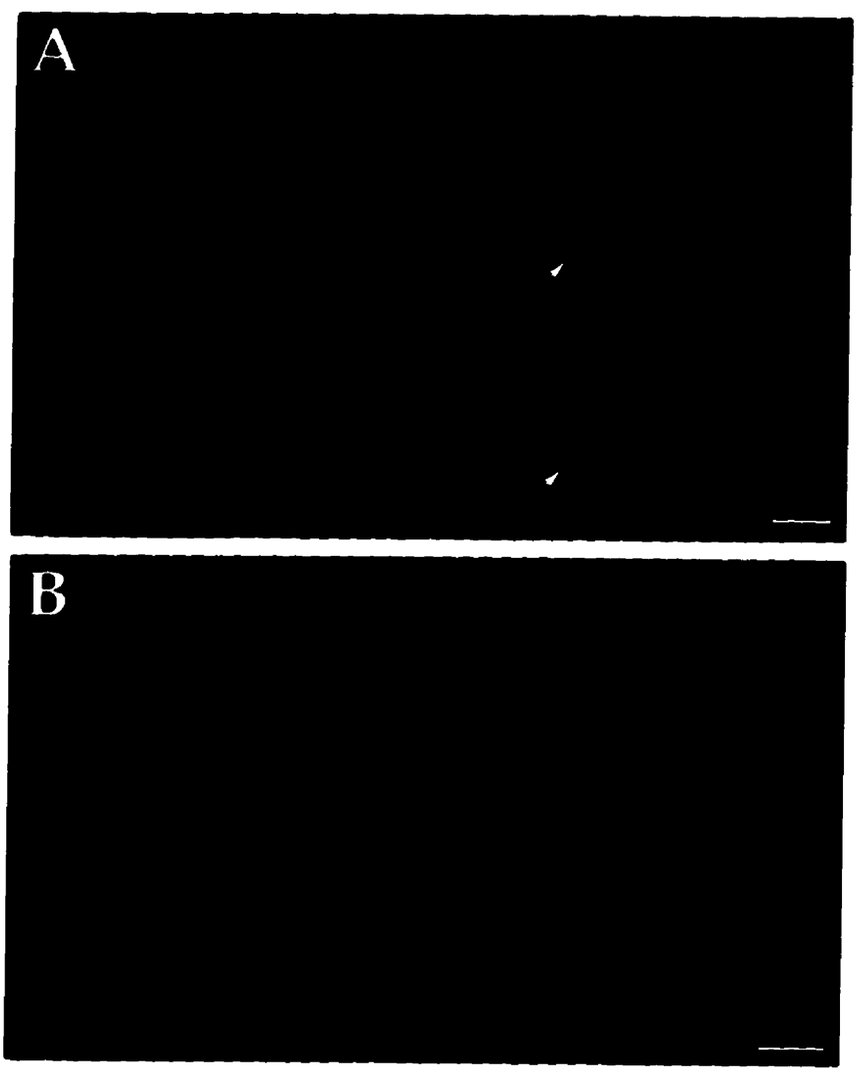
A
B

Figure 15. Examples of BrdU-NeuN- and BrdU-Calbindin-immunoreactive cells in the dentate gyrus.

(A,B) Two photomicrographs of BrdU-IR cells (processed at 6 weeks) that are NeuN-IR (A and B, long arrows) and non-NeuN-IR (A, short arrow) in the dentate gyrus.

(C-H) Two series of photomicrographs (C-E and F-H) showing BrdU-IR nuclei (C and F) in the same field and plane of focus with Calbindin-IR cells (D and G), are combined to produce BrdU-Calbindin double labeled cells in the infrapyramidal (E) and suprapyramidal (H) limbs of the dentate gyrus (processed at 6 weeks). Note: (i) the difference in size of BrdU-IR cells in (A) that are (long arrow) and are not (short arrow) NeuN-IR, (ii) doublet of BrdU-IR cells (short arrow, A), and (iii) the mottled appearance of BrdU-IR cells in C and E, and F and H. Scale bar in B = 20 μm, and applies to frames A and B; bar in H = 20μm and applies to frames C through H.

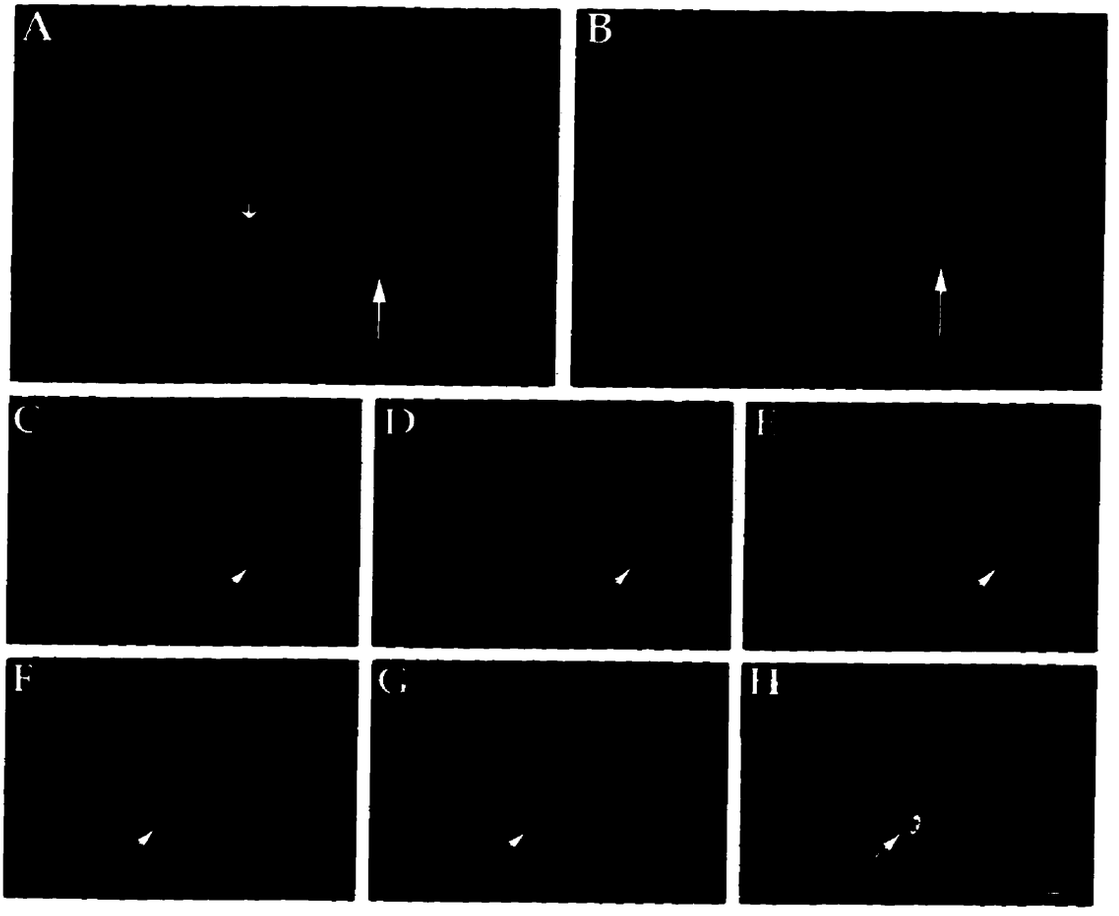
A
B
C
D
E
F
G
H

more differentiated (i.e. exhibited mature neuronal or glial cell markers), the pattern of fluorescence changed from completely filling the nucleus (short arrow, Figure 15A), to becoming what Nowakowski and Miller (1988) described as "mottled" in appearance (green cells without arrows, Figure 15 C and F). That is, bright spots of BrdU-immunofluorescence overlaying a "background" of moderate BrdU-immunofluorescence. These two characteristics, larger nuclei and "mottled" BrdU-immunofluorescence, were relatively consistent indicators of more differentiated cell types. Figure 15 A (short arrow) also illustrates a possible doublet of BrdU-IR cells in the crest region of the hilus of the dentate gyrus. As previously described, the incidence of mitotic doublets throughout the hippocampus was highest in this region (i.e. immediately adjacent to the granule cell layer).

3.3.3 *BrdU-immunoreactive cells differentiate into neurons and glia in Ammon's horn.*

As in the region of the dentate gyrus, BrdU-NeuN- and BrdU-GFAP-IR cells were first detected in Ammon's horn 3 weeks following the administration of the nucleotide (Figure 16). Once again the percentages of BrdU-GFAP-IR cells remained basically unchanged, while the percentage of BrdU-NeuN-IR cells declined significantly as survival times increased from 3 weeks (~24%) to 24 weeks (~3.7%) ($p<0.01$; two tailed T-Test). A comparison of the percent of double-labeled cells in Ammon's horn versus the dentate gyrus suggests that: (i) approximately the same percentage (~10%) of BrdU-GFAP-immunoreactive

Figure 16. Over time BrdU-immunoreactive cells express neuronal and glial antigens in the region of Ammon's horn.

Percentage of BrdU-IR cells in Ammon's horn which were NeuN-IR (solid bar) and GFAP-immunoreactive (stippled bar) at various survival times following the administration of BrdU. A comparison of the number of double-labeled cells at 3 weeks and 24 weeks reveals no significant difference in the percentage of BrdU-GFAP-IR cells, but a significant decline in the percentage of BrdU-NeuN-IR cells ($p<0.01$; two tailed T-test). Error bars represent mean + S.D.

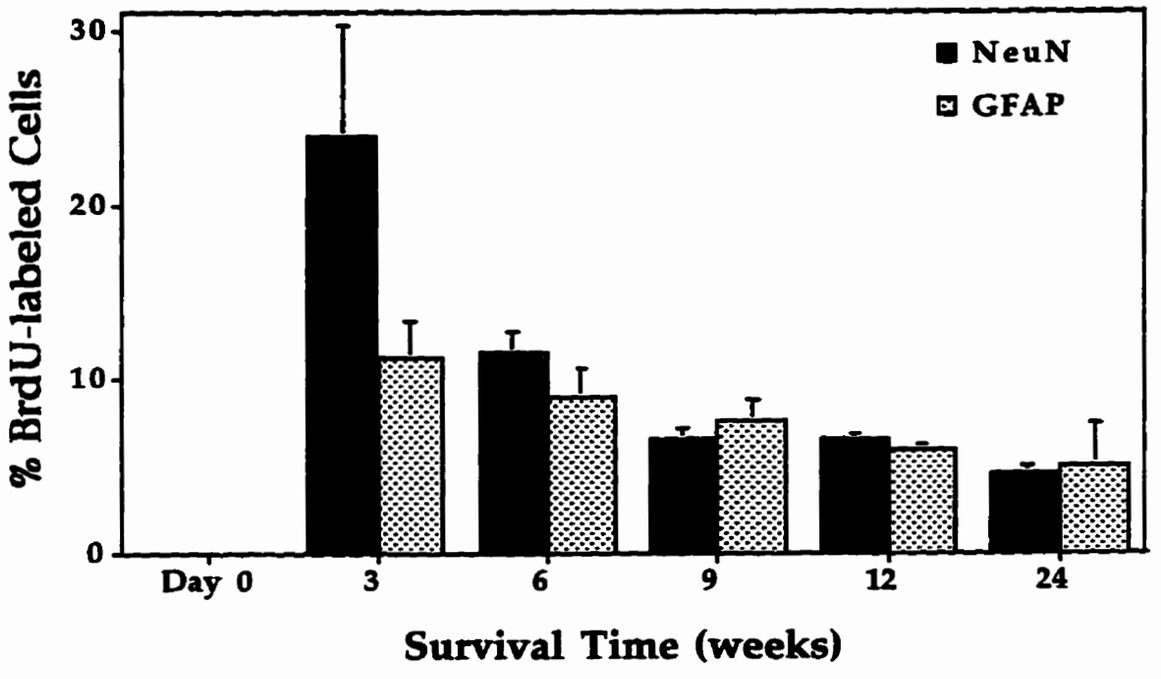
30
20
10
0
% BrdU-labeled Cells
NeuN
GFAP
Day 0
3
6
9
12
24
Survival Time (weeks)

cells were detected in both regions while, (ii) a much greater percentage of BrdU-NeuN-IR cells were detected in the dentate (3 wks~58.6%, 24 wks~20.2%) versus Ammon's horn (3 wks~24%, 24 wks~4.6%) (Figures 13 and 16).

The majority of BrdU-GFAP and BrdU-S-100-IR cells were located in stratum radiatum and stratum lacunosum moleculare (Figure 17). Although double-labeled glial cells were also detected in stratum oriens, no such cells were observed at any time in the pyramidal cell layer. The morphology of the BrdU-GFAP-IR cells once again resembled that of mature astrocytes, exhibiting characteristic stellate processes extending from the BrdU- IR nucleus (Figure 17 B-D).

Unlike newly-generated glial cells, the majority of the BrdU-NeuN-IR cells were located in close approximation, or directly within the pyramidal cell layer (Figure 18). Owing to the larger area of the CA1 region as compared to CA2-3, a slightly greater number of BrdU-NeuN-IR cells were found in the region of CA1 (data not shown). As previously described, the BrdU-IR nuclei of NeuN-IR cells in Ammon's horn were generally larger and exhibited a "mottled" appearance in comparison to those which did not exhibit NeuN-immunoreactivity, however, this was not always the case (Figure 18 D and F). Owing to the close approximation of NeuN-IR cells in the pyramidal cell layer, a second neuronal label was employed. Only a single example of a BrdU-Calbindin-IR cell was found in the CA1 pyramidal cell layer following the examination of two animals at each of the 5 survival times (Figure 19).

Figure 17. Examples of BrdU-S-100- and BrdU-GFAP-immunoreactive cells in Ammon's horn.

(A) Photomicrograph of a BrdU-S-100-IR cell (processed at 6 weeks) in stratum radiatum of CA1.

(B-D) A series of photomicrographs (processed at 6 weeks) showing a BrdU-IR nucleus (B) in the same field and plane of focus with a GFAP-IR cell (C) which are blended to produce a BrdU-GFAP-IR cell (D) in stratum lacunosum moleculare of CA1. Scale bar in A = 10 μm; bar in D = 10μm and applies to frames B through D.

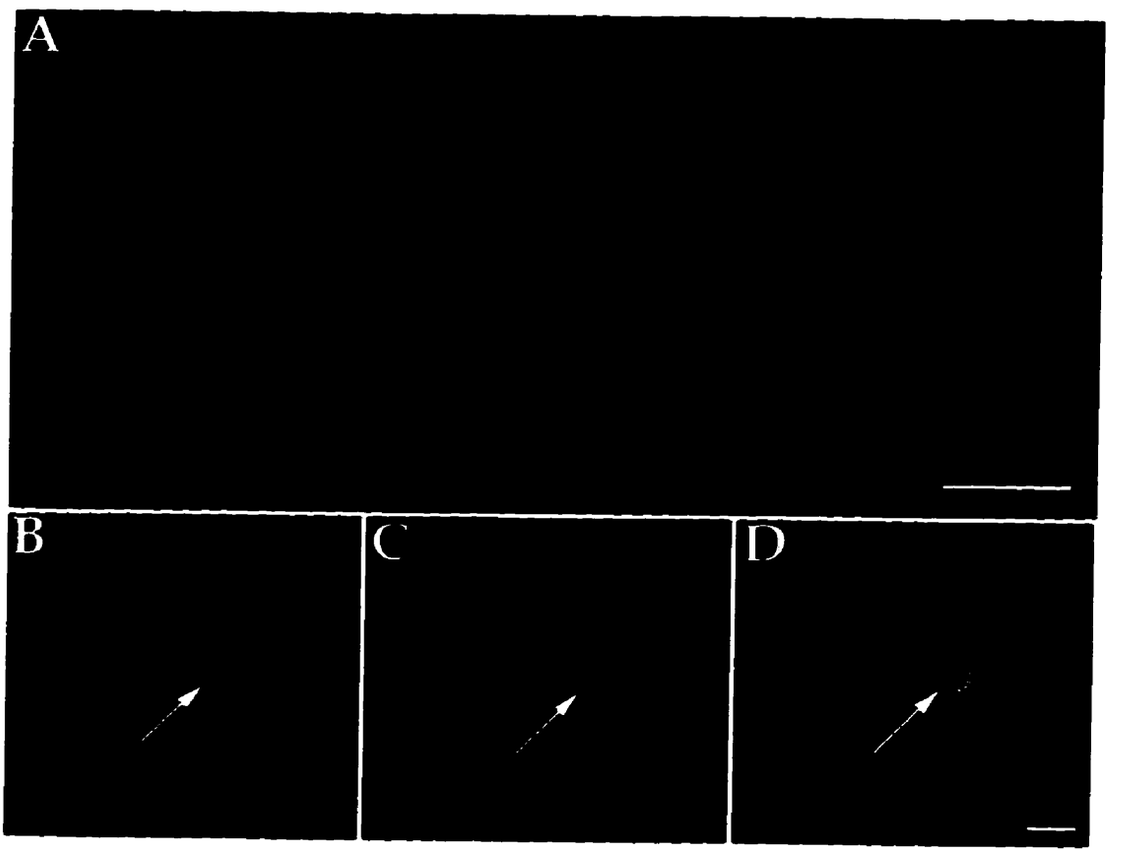
A
B
C
D

Figure 18. Examples of BrdU-NeuN-immunoreactive cells in Ammon's horn.

Three series of photomicrographs (A-C, D-F, and G-I) (processed at 6 weeks) showing BrdU-IR nuclei (A, D, G) in the same field and plane of focus with NeuN-IR cells (B, E, H). These are combined to produce BrdU-NeuN-IR cells in stratum pyramidal (C) and stratum oriens (F) of CA1, and stratum pyramidal (I) of CA3. Scale bar in I = 20 μm, and applies to all frames.

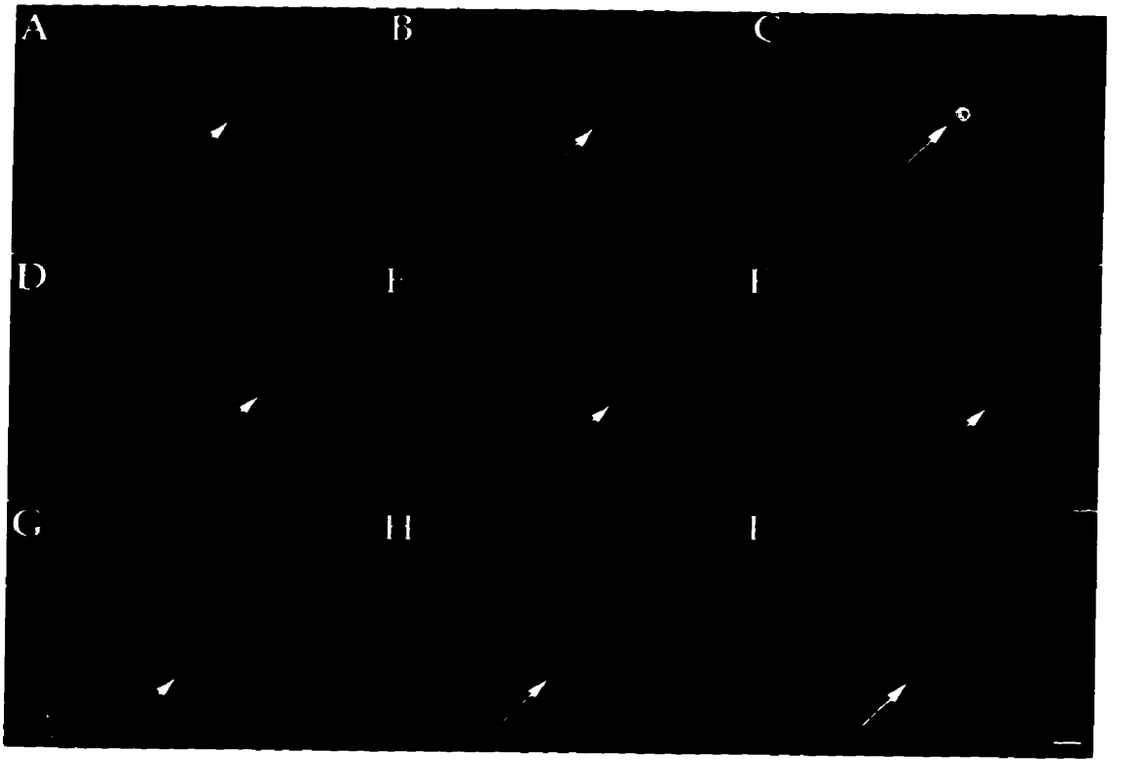
A
B
C
D
E
F
G
H
I

Figure 19. An example of a BrdU-Calbindin-immunoreactive cell in the CA1 pyramidal cell layer of Ammon's horn.

A photomicrograph (processed at 6 weeks) of two Calbindin-IR cells (red), with only one displaying a BrdU-IR (arrow) nucleus in the CA1 pyramidal cell layer of Ammon's horn. Note the presence of basal dendrites in both cells. Scale bar = 20 μm.

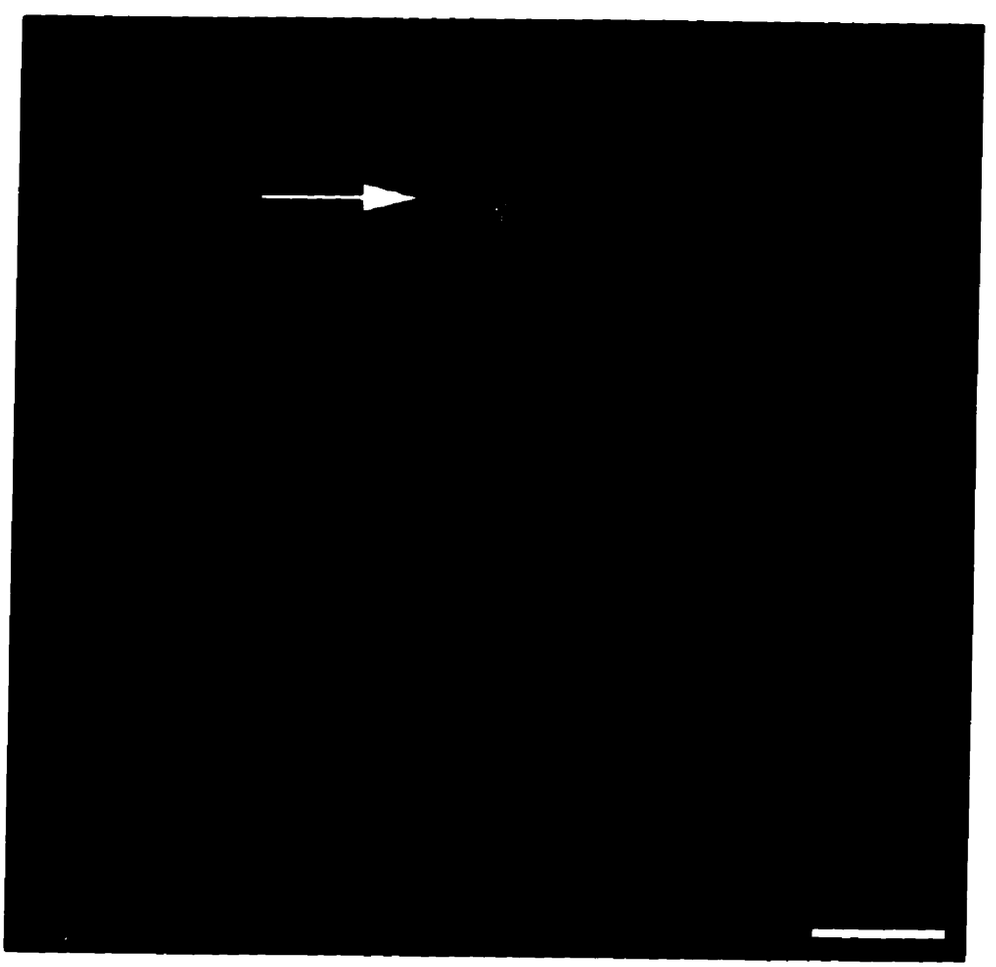

4.0 DISCUSSION

The results of this study indicate for the first time, that the generation of new neurons and glia in the adult mammalian hippocampus is not limited to the region of the dentate gyrus, but rather extends into Ammon's horn. Identification of these newly-generated cells was made possible by employing a novel BrdU-labeling protocol. This protocol attempted to account for cytokinetic changes such as increased cell cycle times and decreased growth fractions which occur in the central nervous system as an animal ages. The distribution of the newly-generated neural cells is suggestive of an interneuronal population, whose presence may serve to modulate synaptic efficacy within the hippocampus without disturbing the circuitry of the system.

4.1 *A novel picture of mitotically-active cells in the adult hippocampus.*

At the onset of this investigation it was hypothesized that a novel picture of mitotic activity in the adult central nervous system could be achieved by accounting for increased cell cycle times and decreased growth fractions. Accordingly, adult mice were administered BrdU at concentrations of 1.8, 9.0, and 18.0 mg/mL every two hours for periods of 12, 24, 48, and 72 hours. Essentially these protocols differed from those previously reported in so much as the window of nucleotide delivery was protracted from a period of hours to a period of days, while still ensuring that the time between injections remained

less than the population's reported S-phase. Figures 6 and 7 illustrate that the results of these protocols were two fold. First, in regions where proliferating cells have previously been reported in the adult (i.e. dentate gyrus), a greater number of BrdU-IR cells were detected. Cameron *et al.* (1993) reported that in a 40 μm coronal section through the dentate gyrus of an adult mouse, the maximum number of [^{3}H]-thymidine-labeled cells was 7. In coronal sections (14 μm) through the same region employing an extended labeling protocol, a maximum of 26 BrdU-IR (Figure 12) and [^{3}H]-thymidine-labeled (Figure 8) cells were detected. Second, BrdU- (Figure 6) and [^{3}H]-thymidine- (Figure 11) IR cells were detected in regions of the hippocampus (i.e. Ammon's horn) not previously reported. number. These results suggest that a greater amount of nucleotide was made available to the proliferating cells for a longer period of time. This facilitated the novel detection of putative slow cycling cells which may have been overlooked in previous investigations due to the sub-threshold levels of the nucleotide being incorporated.

The possibility does exist that the increased number of BrdU-IR cells (discussed below) observed in regions of the hippocampus where proliferation has been previously described (i.e. dentate gyrus) could be related to stressing the animals. Morshead and van der Kooy (1992) reported that animals which were stressed by administering anesthetic 24 hours before labeling, displayed more [^{3}H]-thymidine-labeled subependymal cells than controls. Although they

noted that the increase in [^{3}H]-thymidine-labeled cells was transient and did not translate into an increase in Nissl stained cells, they could not discount the immediate effects stressing the animal had on [^{3}H]-thymidine-labeled cell

In the BrdU incorporation study, two protocols (1.8 mg/mL over 72 hours; 9.0 mg/mL over 48 hours) resulted in the detection of an equivalent number of cells (97± 9 and 96 ± 8 respectively) (Figure 7). Although either protocol could have been used to investigate the identity of the BrdU-IR cells, the latter method was selected for two principle reasons. First, as higher concentrations of BrdU were employed to detect the proliferating cells, a leveling off in cell number was apparent at earlier time points (Figure 7). This leveling off could possibly be attributed to: (a) the cytotoxic effect of the nucleotide, or (b) the identification of more than one population of proliferating cells. If more than one populaiton of cells was detected, (with one population of being characterized by a longer cell cycle time) a leveling off in cell number would be apparent (Morshead *et al.*, 1992). However, a stalling of the cell cycle or inhibition of proliferation, (both caused by cytotoxicity) could also explain this finding. Because the cytotoxic effects of continuously administering the nucleotide are more pronounced over time, (even though we did not assay for them) any detection method which detects an equivalent number of cells in a shorter time frame would be preferred. Second, the BrdU-IR cells detected with 1.8 mg/mL were more difficult to detect. This problem in detection would only become more

pronounced as survival times increased, and would make the future identification of double-labeled cells nearly impossible. The difficulty with detection of the proliferating cells when the lowest concentration of BrdU was employed is suggestive of why previous investigators failed to detect mitotically-active cells outside the dentate gyrus. Proliferating cells may have been missed when either sub-threshold levels of the nucleotide were present over an extended time course (as in our case), or supra-threshold levels of the nucleotide were present over an inadequate amount of time (pulse techniques). In both cases, proliferating cells were unable to incorporate adequate amounts of the nucleotide during S-phase, so as to rise above the threshold of detection.

4.2 *The BrdU incorporation seen after extended labeling periods is likely not due to polyploidy or DNA repair.*

We propose that the administration of 9.0 mg/mL (45 mg/kg B.W.) of BrdU every two hours for 48 hours resulted in BrdU-IR cells being detected in greater numbers (Figure 7) and in regions of the hippocampus not previously reported (Figures 6). However, the possibility exists that these were not proliferating cells, but rather cells in which the process of polyploidization or DNA repair was occurring.

Polyploidy is a state of having more than two full sets of homologous chromosomes, and occurs as a consequence of blocking the normal course of

mitosis at various levels (Vendrely and Vendrely, 1956; Mazur, 1990; Nagl, 1990). This phenomenon is more typical of plants and invertebrates than vertebrates, however, the incidence of polyploidy in mammalian cells has been reported in the liver (Goss, 1967), urinary bladder (Walker, 1959), salivary glands (Redman and Sreebny, 1970), pancreas (Pictet *et al.*, 1972), duodenum (Troughton and Trier, 1969), and in megakaryocytes of bone marrow (Medvedev, 1986).

It is unlikely that polyploidization is responsible for the detection of BrdU-IR cells in the hippocampus for the following reasons. First, the majority of the mammalian cell types exhibiting polyploidy are established by the cell failing to accomplish mitotic telophase (i.e. divide) (Carriere, 1967; Winkelmann *et al.*, 1987). This failure results in two pairs of sister chromatids remaining within one cell, and upon reformation of the nuclear membrane, the formation of binucleate cells. Although the occurrence of two BrdU-IR nuclei in close approximation (a possible binucleate cell) was noted in this study, the vast majority of the labeled nuclei were not in close approximation, discounting the premise that the cells are polyploidy (Figure 6). Second, due to the increased DNA content of polyploid cells, the nuclei of such cells are usually greater in diameter than proliferating cells (Cogeshall *et al.* , 1970; Lasek and Dower, 1971; Brodsky and Uryvaeva, 1977). The BrdU-IR cells examined at day zero all appear to be approximately 5 μm in diameter (Figure 6). Third, previous studies examining the occurrence of mitotically-active cells in the adult hippocampus

using both [^{3}H]-thymidine and BrdU have failed to detect such cells outside the dentate gyrus. If polyploidization was occurring, at least one investigation in the past 35 years should have noted the occurrence of mitotically-active cells. Finally, to date only one example of a mature CNS cell containing more than two sets of the haploid genome has been demonstrated. Lapham *et al.* (1971) reported the unusual occurrence of an intermediate amount of DNA (between 2 and 4 haploid units) in the Purkinje neuron of the rat cerebellum. This uncommon phenomenon was thought due to the partial replication of the genome at some stage of development, and has not been reported to occur in any other CNS cell type.

Because we have not completed an investigation into the occurrence of polyploidy in the BrdU-IR cells ourselves, we can not completely eliminate the possibility of its occurrence. However, it seems unlikely given the arguments listed above that the incorporation of BrdU reported in this study is due to polyploidization.

In general, DNA damage and subsequent repair can occur in either proliferating (which will be discussed later) or non-proliferating populations of cells (Barnes *et al.*, 1993). DNA damage in non-proliferating cells can be caused either by intrinsic factors, or as a consequence of external factors such as exposure to ultraviolet radiation, metabolizing enzymes, or other toxic chemicals (Baan, 1987). In the majority of cases response to the damage requires

nucleotide excision repair, where the defective DNA is cut out and replaced with undamaged nucleotides through DNA synthesis and ligation (Naegeli, 1995). If the repair process occurs in the presence of BrdU or [^{3}H]-thymidine and these nucleotides are incorporated, the non-proliferating cell will appear mitotically-active (Howard-Flanders, 1973; Hanawalt *et al.*, 1979).

In such cases, you would expect to see the scattered appearance of BrdU-IR loci within a relatively unlabeled nucleus. This is due not only to the frequency of repair, but also because only one nucleotide of a possible four which can be employed in the repair process (in the case of BrdU) will be detected. In hippocampal sections processed for BrdU-immunocytochemistry immediately following the completion of the labeling protocol, all of the nuclei exhibiting BrdU-immunoreactivity did so in an "all or none" fashion (Figure 6). That is to say, the entire nucleus was either bright with the fluorescently tagged marker or no nucleotide was detected, the scattered labeling pattern indicative of DNA repair was not observed. At survival times of 3 weeks cells with mottled BrdU-IR nuclei were observed, suggesting that cell division rather than DNA repair had taken place, diluting the level of incorporated nucleotide. If DNA damage existed to the extent that the entire nucleus was BrdU-IR we would expect that, rather than attempt to repair the damage and risk mutagenesis, the cell would undergo apoptosis.

4.3 *A comparison with lower concentrations of [^{3}H]-thymidine suggests that the BrdU-labeling protocol does not produce any discernable cytotoxic effects.*

Having addressed the possibility that BrdU-incorporation was due to a non-proliferative event, it is important to establish that the incorporation of nucleotide into the proliferating cells did not cause a cytotoxic effect. The exposure of tissue cultures to high concentrations of [^{3}H]-thymidine and/or BrdU has been shown to cause a gradient of cytotoxic effects. These effects are progressively manifested through: (i) the slowing or stalling of the cell cycle (usually in S-phase), (ii) inhibition of proliferation, (iii) early or inappropriate differentiation, (iv) irreversible chromosomal damage, and finally (v) cell death via apoptosis (Cleaver, 1967; Sawicki and Dorn, 1973; Kufe *et al.*, 1980; Maurer, 1981; Trent *et al.*, 1986; Miller and Nowakowski, 1988). Numerous investigators have worked to determine the acceptable levels of exogenous nucleotides in culture (reviewed in Feinendegen, 1967). However, it is difficult (if not impossible) to relate *in vitro* data to investigations performed *in vivo*. Therefore, to demonstrate that the BrdU injection protocol did not cause a toxic effect we compared the number and distribution of BrdU-IR cells with a separate group of animals which received 0.10 mL i.p. injections of 10 mg/kg B.W. [^{3}H]-thymidine (8.33μCi/injection; specific activity = 6.7 Ci/mmol). Previous investigations (reviewed in section 2.1.2) have indicated that this concentration and specific activity does not produce discernible toxic effects.

Comparison of the number (Figure 7) and distribution of BrdU versus [^{3}H]-thymidine-labeled cells suggests that the BrdU-labeling protocol does not produce a stalling or inhibition of the cell cycle in proliferating cells. Evidence of such an event would be manifested through: (a) a disparity in the overall distribution of BrdU versus [^{3}H]-thymidine-labeled cells, (b) an absence of BrdU-labeled mitotic doublets, or (c) an absence of BrdU-labeled mitotic doublets in regions containing [^{3}H]-thymidine-labeled mitotic doublets, and (d) greater numbers of [^{3}H]-thymidine versus BrdU-labeled cells in at least one region of the hippocampus. [^{3}H]-thymidine consistently detected significantly fewer cells in all regions of the hippocampus (Figure 8). However, in every region where BrdU-IR cells or mitotic doublets were detected, [^{3}H]-thymidine-labeled cells and mitotic doublets were also observed (Figures 9, 10, 11). This can't be attributed to the relative sensitivities of the respective nucleotides, nor to differences in their permeablities through the blood brain barrier (the choroid plexus), since it has been established that both nucleotides are virtually identical in both regards (Packard *et al.*, 1973; Raza *et al.*, 1985; Nowakowski *et al.*, 1989; Morris, 1991). However, it is possible that the reduced number of [^{3}H]-thymidine-labeled cells could be due to the fact that a lower amount of the nucleotide was employed as compared to that of BrdU. To test this hypothesis, a second set of animals injected with a higher dose of [^{3}H]-thymidine (closer to that of BrdU) could have been used. Then, by following the three groups of

animals (BrdU, [^{3}H]-thymide low concentration, [^{3}H]-thymidine higher concentration) over 3, 6, 9, 12, and 24 weeks, a more distinct picture of differentiation, proliferation, and cytotoxicity could be achieved.

The results presented in Figure 7 also suggest that the BrdU-labeling protocol did not produce a toxic effect, in so much as altering the proliferative capacity of the labeled cells. Recall that as increasing concentrations of BrdU were used, a plateau in the number of labeled cells became noticeable. In each case an almost linear increase in the number of labeled cells preceded the plateau, indicating the approximate point at which toxicity of the nucleotide caused an inhibition in proliferation. At 48 hours the number of labeled cells using 9.0 mg/mL still represents a linear increase, suggesting that stalling or inhibition of the cell cycle has not occured.

4.4 *Evidence for newly-generated neurons and glia throughout the hippocampus.*

To determine the number, distribution, and fate of the BrdU-IR cells following the administration of the nucleotide, three animals were perfused at survival times of 3, 6, 9, 12, and 24 weeks. Quantitative analysis of the BrdU-IR cells revealed a significant decline in the number of cells detected between day zero and 24 weeks (Figure 12). This decline occurred both in Ammon's horn and the dentate gyrus, and can be attributed to three possible mechanisms; cell death, proliferation, and migration. Although each possibility has the potential

to account for the decline, the most plausible explanation is that combination of the three is occurring. Previous studies have illustrated the proliferation of [^{3}H]-thymidine-labeled precursors in the dentate gyrus, followed by their migration and differentiation into neurons and glia supporting the possibility that such a combination of processes is occurring here (Gueneau *et al.*, 1982; Kaplan and Bell, 1984; Stanfield and Trice, 1988; Cameron *et al.*, 1993) However, if all the of BrdU-IR cells detected at day zero (estimated at 14,400) proceed ed to divide and give rise to new neurons and glia, one would expect a significant increase in the size and density of the hippocampus in the mouse over time. Especially since multiple divisions would be necessary in numerous cases so as to dilute the level of incorporated nucleotide to sub-threshold levels. Since no such increase is apparent, the fate of the majority of the BrdU-IR cells must be death. However, as illustrated by the consistent number of BrdU-IR cells detected between 3 and 24 weeks, not all the proliferating cells undergo cell death (Figure 12).

Double-label immunocytochemistry performed on the BrdU-IR cells in the dentate demonstrated the presence of mature neural antigens at 3 weeks (Figure 13). The majority of the BrdU-IR cells differentiated into committed neurons (NeuN, Calbindin; Figure 15), while a smaller portion presented glial antigens (S-100, GFAP; Figure 14). The time course of antigen presentation was similar to previously reported works, as was the proportion of neurons as compared to

glia. Cameron *et al.* (1993) demonstrated that (in the rat) immediately following the labeling of dividing cells, positive immunoreactivity for mature neurons (NSE) or glia (GFAP) was absent. However, at three weeks the majority (approx. 70%) of labeled cells were NSE immunoreactive, while approximately 10% were GFAP-immunoreactive. In both studies, the distribution of GFAP-labeled cells occurred primarily outside the granule cell layer, while the majority of newly-generated neurons were located within the granule cell layer. Because of this phenomena, two neuronal markers were employed in this study. NeuN, which recognizes a neuronal specific nuclear protein, and Calbindin, which recognizes a neuron-specific calcium binding protein typically found in dentate gyrus granule cells (Sloviter, 1989; Celio, 1990). Both identified BrdU-labeled cells of similar morphology and distribution.

The generation of new neurons and glia in the region of the dentate gyrus have been reported previously and investigated in greater detail than in the present study. Therefore, the discussion concerning the location, morphology, and other attributes concerning the generation of new cell types in the adult will be limited to the region of Ammon's horn.

The results presented in this study suggest that new neurons and glia are being generated in the region of Ammon's horn of the adult mouse, a finding not previously reported. A comparison of the number of BrdU-GFAP-IR cells in the region as a function of survival time (Figure 16) reveals that: (i) GFAP

immunoreactivity is initially detected at three weeks, and (ii) the percentage of BrdU-GFAP-immunoreactive cells does not change significantly between 3 and 24 weeks. This suggests that BrdU-GFAP-IR cells do not undergo proliferation or cell death to a significant degree, but rather differentiate into functional post-mitotic astrocytes, as evidenced by their characteristic GFAP-immunoreactivity, and bright BrdU fluorescence. These observations seem to indicate that a slow but steady rate of glial cell turnover is occuring in Ammon's horn.

In contrast to the pattern previously described, the percentage of BrdU-NeuN-IR cells declined significantly between their first occurrence (3 weeks) and the latest time point examined (24 weeks) (Figure 16). This decline in cell number can be interpreted in three ways. The first and simplest explanation is that at some point after the BrdU-IR cells divided and differentiated into BrdU-NeuN-IR cells they underwent cell death and were removed. The second and third explanations are related to the neuronal marker NeuN. The expression of the antigen which is recognized by NeuN has been demonstrated to appear as early as E 9.5 in the neural tube of the mouse (Mullen *et al.*, 1992). The time of appearance and position of the NeuN-IR cells coincides closely with the first-born neurons of the mouse neural tube (Nornes and Carry, 1978; McConnell, 1981). However, it is likely that a portion of the labeled cells in the neural tube are still capable of proliferation. Therefore, putative proliferation of the BrdU-NeuN-IR cells detected at three weeks could cause the dilution of the incorporated nucleotide, and result in a decline in the number of double-labeled

cells being detected. So, it is possible that those cells initially detected at three weeks could proliferate, diluting the nucleotide and subsequently: (a) undergo cell death, or (b) remain as fully functional neurons whose BrdU-immunoreactivity has fallen below detectable levels.

While it is likely that a combination of the three processes described above are occuring, it is impossible to determine which process specific populations of cells are undergoing. Noteably, three lines of evidence suggest that a portion of the BrdU-NeuN-IR cells remain in the region of Ammon's horn. First, the observation that the majority of the BrdU-NeuN-IR cells displayed a "mottled" appearance suggests that cell division has occurred. Second, the occurance of BrdU-NeuN-IR cells at every time point after their initial detection and third, the demonstration of a BrdU-Calbindin-IR cell indicates that post-mitotic neurons persist in Ammon's horn for an extended period of time.

The observation that the majority of the newly-generated neurons are located in stratum radiatum and in close approximation or directly within the pyramidal cell layer of Ammon's horn suggest that we are dealing with the generation of interneurons. The occurance of Calbindin-IR interneurons have previously been described in stratum radiatum and the region of the pyramidal cell layer boarding stratum radiatum (Sloviter, 1989). This suggests the possibility that the BrdU-Calbindin-IR cell observed in this study is an interneuron (Figure 19). Functionally, the addition of interneurons to the existing circuitry of the hippocampus makes sense. Rather than disturb

established projection pathways, modulation or alteration of input could be accomplished through the addition or replacement of local interneurons. This scenario has been demonstrated to occur in the dentate gyrus and olfactory bulb of the adult mouse (reviewed in Altman and Bayer, 1993 and Rousselot *et al.*, 1995). In both cases, the generation of locally projecting granular neurons (or interneurons) continues throughout the life of the animal. In the case of the dentate gyrus, neurogenesis is regulated in part by adrenal steroids, excitatory input, and NMDA receptor activation (Gould *et al.* , 1990; Gould *et al.* , 1992; Gould and McEwen, 1993; Cameron and Gould, 1994; Cameron *et al.*, 1995). This arrangement allows for the maintenance of appropriate hippocampal function, while providing a means through which synaptic efficacy can be modulated. An alternative explanation of the single BrdU-Calbindin-IR cell is that "one equals none". That is, the occurance of the BrdU-Calbindin-IR cell is not real. To test for this hypothesis, one could assay for the presence of putatative BrdU-IR interneurons by employing an anti-GABA immunocytochemical label in conjunction with BrdU immunoreactivity, since the majority of interneurons are GABAergic in Ammon's horn.

The observation that the majority of newly-generated glia in Ammon's horn are localized in stratum radiatum and stratum lacunosum moleculare is also consistent with this model of altering synaptic efficacy. The Hebbian model of alter synaptic efficacy states that "When an axon of cell A...excite[s] cell B and repeatedly persistently takes part in firing it, some growth process or metabolic

change takes place in one or both cells so that A's efficiency as one of the cells firing B is increased." (Hebb, 1949). In Ammon's horn, the most attractive region to alter synaptic efficacy with minimal disturbance would seem to be in the dendritic fields of the pyramidal neurons (i.e. stratum radiatum and stratum lacunosum moleculare). This modulation could be accomplished through the addition of astrocytes or neurons, both of which have been reported in this study.

Throughout the investigation a population of BrdU-IR cells, did not exhibit either neuronal or glial antigens (data not shown). The majority of these BrdU-IR cells are small (approx. 5 μm) and are characterized by a full, bright pattern of fluorescence, indicating that they have not diluted the level of incorporated nucleotide. Their preferential location in the subgranular zone of the dentate gyrus is suggestive of a putative progenitor population as described in Kuhn *et al.* (1996). However, their small size and bright pattern of fluorescence could also be indicative of microglia or macrophages which have been described throughout the CNS (Perry *et al.*, 1985; Leong and Ling, 1992).

SUMMARY AND FUTURE DIRECTIONS

Through the development of a novel labeling protocol we have demonstrated the widespread generation of new neurons and glia in the hippocampus of the adult mouse. We further demonstrated for the first time,

that neuro- and gliogenesis is not restricted to the region of the dentate gyrus, as previously thought, but occurs in Ammon's horn. The distribution of new neurons and glia is consistent with locations of modified synaptic efficacy in the hippocampus, suggesting a possible role for the newly-generated cells in the processing of new information. Several questions still remain unanswered. For example, what percentage of newly-generated neurons and glia undergo cell death? What is the significance and/or functional consequence of a population of cells in the hippocampus turning over? Are there progenitor or stem cells in the region of the hippocampus which give rise to these new cells? What factors control the processes of neuro- and gliogenesis in the region? Is this phenomena simply a continuation of the prolonged development of the hippocampus?

Answers to questions such as these may provide a better understanding of the role of cell turnover in hippocampal function. Understanding what controls this process may allow for stimulated repair of the hippocampus after injury or disease.

REFERENCES

Alkon, D.L., Amaral, D.G., Bear, M.F., Black, J., Carew, T.J., Cohen, N.J., Disterhoft, J.F., Eichenbaum, H., Golski, S., Gorman, L.K. (1991). Learning and memory. *Brain Res. Rev.* **16**: 193-220.

Altman, J. (1963). Autoradiographic investigation of cell proliferation in the brains of rats and cats. *Anat. Rec.* **145**: 573-591.

Altman, J. (1966). Autoradiographic and histological studies of postnatal neurogenesis. II. A longitudinal investigation of the kinetics, migration and transformation of cells incorporating tritiated thymidine in infant rats, with special reference to postnatal neurogenesis is some brain regions. *J. Comp. Neurol.* **128**: 431-474.

Altman, J. and Bayer, S.A. (1990a). Mosaic organization of the hippocampal neuroepithelium and the multiple germinal sources of dentate granule cells. *J. Comp. Neurol.* **301**: 325-342.

Altman, J. and Bayer, S.A. (1990b). Prolonged sojourn of developing pyramidal cells in the intermediate zone of the hippocampus and their settling in the stratum pyramidale. *J. Comp. Neurol.* **301**: 343-364.

Altman, J. and Bayer, S.A. (1990c). Migration and distribution of two populations of hippocampal granule cell precursors. *J. Comp. Neurol.* **301**: 365-381.

Altman, J. and Bayer, S.A. (1993). Are new neurons formed in the brains of adult mammals? In: Cuello, A.C. (ed) *Neuronal Cell Death and Repair*. Elsevier Science Publishers. New York. pp. 203-225.

Altman, J. and Das, G.D. (1965). Autoradiographic and histological evidence of postnatal hippocampal neurogenesis in rats. *J. Comp. Neurol.* **124**: 319-336.

Altman, J. and Das, G.D. (1966a). Autoradiographic and histological studies of postnatal neurogenesis. I. A longitudinal investigation of the kinetics, migration and transformation of cells incorporating tritiated thymidine in neonate rats, with special reference to postnatal neurogenesis is some brain regions. *J. Comp. Neurol.* **126**: 337-390.

Altman, J. and Das, G.D. (1967). Post-natal neurogenesis in the guinea-pig. *Nature* **204**: 1098-1101.

Amaral, D.G. (1978). A Golgi study of cell types in the hilar region of the hippocampus of the rat. *J. Comp. Neurol.* **182**: 851-914.

Amaral, D.G. and Witter, M.P. (1989). The three-dimensional organization of the hippocampal formation. A review of anatomical data. *Neuroscience* **31**: 571-591.

Ambercrombie, M. (1946). Estimation of nuclear population from microtome sections. *Anat. Rec.* **94**: 239-247.

Anderson, P. (1975). Organization of hippocampal neurons and their interconnections. In: Isaacson, R.L. and Pribram K.H. (eds) *Structure and Development*. Plenum, New York, pp. 155-175. (The hippocampus, vol. 1).

Angevine, J.B. (1963). Autoradiographic study of histogenesis in the hippocampal formation of the mouse. *Anat. Rec.* **145**: 201.

Angevine, J.B. (1964). Autoradiographic study of histogenesis in the area dentata of the cerebral cortex in the mouse. *Anat. Rec.* **148**: 255.

Angevine, J.B. (1965). Time of neuron origin in the hippocampal region. An auto-radiographic study in the mouse. *Exp. Neurol. Suppl.* **2**: 1-70.

Angevine, J.B. (1975). Development of the hippocampal region. In: Isaacson, R.L., Pribram, K.H. (eds) *Structure and Development*. Plenum, New York, pp. 61-94 (The hippocampus, vol. 1).

Ashwood, T.J., Lancaster, B. and Wheal, H.V. (1984). In vivo and in vitro studies on putative interneurones in the rat hippocampus: Possible mediators of feed-forward inhibition. *Brain Res.* **293**: 279-291.

Atlas, M. and Bond, V.A. (1965). Time of neuron origin in the hippocampal region: an autoradiographic study in the mouse. *J. Cell Biol.* **26**: 19-24.

Baan, R.A. (1987). DNA Damage and Cytogenic End Points. In: Obe, G., Basler, A. (eds) *Cyto-genetics*. Springer-Verlag, Berlin pp. 327-344.

Bannister, N.J. and Larkman, A.U. (1995a). Dendritic morphology of CA1 pyramidal neurones from the rat hippocampus: I. Branching patterns. *J. Comp. Neurol.* **360**: 150-160.

Bannister, N.J. and Larkman, A.U. (1995b). Dendritic morphology of CA1 pyramidal neurones from the rat hippocampus: II. Spine distributions. *J. Comp. Neurol.* **360**: 161-171.

Barnes, D.E., Lindahl, T., and Sedgwick, B. (1993). DNA repair. *Curr. Opin. Cell Biol.* **5**: 424-433.

Bayer, S.A. (1980a). Development of the hippocampal region in the rat. I. Neurogenesis examined with 3H-thymidine autoradiography. *J. Comp. Neurol.* **190**: 87-114.

Bayer, S.A. (1980b). Development of the hippocampal region in the rat. II. Morphogenesis during embryonic and early postnatal life. *J. Comp. Neurol.* **190**: 115-134.

Bayer, S.A. (1982). Changes in the total number of dentate granule cells in juvenile and adult rats: a correlated volumetric and [^{3}H] thymidine autoradiographic study. *Exp. Brain Res.* **46**: 315-323.

Bayer, S.A. (1985). Hippocampal region, In: Paxinos, G. (ed)*The Rat Nervous System.* Academic Press, Australia. pp. 335-352.

Bayer, S.A. and Altman, J. (1974). Hippocampal development in the rat: cytogenesis and morphogenesis examined with autoradiography and low level X-irradiation. *J. Comp. Neurol.* **158**: 55-58.

Bayer, S.A. and Altman, J. (1975). Radiation induced interference with postnatal hippocampal cytogenesis in rats and its long-term effects on acquisition of neurons and glia. *J. Comp. Neurol.* **163**: 1-20.

Bayer, S.A., Altman, J., Russo, R.J., and Zhang, X. (1993). Timetables of neurogenesis in the human brain based on experimentally determined patterns in the rat. *Neurotoxicology* **14**: 83-144.

Blackstad, T.W. (1956). Commisural connections of the hippocampal region in the rat, with special reference to their mode of termination. *J. Comp. Neurol.* **105**: 417-537.

Boss, B.D., Peterson, P.T., and Cowan, W.M. (1985). On the number of neuronal cells in the dentate gyrus of the rat. *Brain Res.* **338**: 144-150.

Braitenberg, V. and Schuz, K. (1983). Some anatomical comments on the hippocampus. In: Seifert, W. (ed) Neurobiology of the Hippocampus. Academic, New York, pp 21-37.

Brodsky, W.Y. and Uryvaeva, I.V. (1977). Cell polyploidy: Its relation to tissue growth and function. *Int. Rev. Cytol.* **50**: 275-332.

Cajal, S. Ramón y (1911). Histologie du systeme nerveux de l'homme et des vertébrés. Vol. 2. Instituto Ramón y Cajal, Madrid.

Cameron, H.A., Woolley, C.S., McEwen, B.S., and Gould,E. (1993). Differentiation of newly born neurons and glia in the dentate gyrus of the adult rat. *Neuroscience* **56**: 337-344.

Cameron, H.A. and Gould,E. (1994). Adult neurogenesis is regulated by adrenal steroids in the dentate gyrus. *Neuroscience* **61**: 203-209.

Cameron, H.A., McEwen, B.S., and Gould,E. (1995). Regulation of adult neurogenesis by excitatory input and NMDA receptor activation in the dentate gyrus. *J. Neurosci.* **15**: 4687-4692.

Cameron, H.A. and Gould, E. (1996). Distinct populations of cells in the adult dentate gyrus undergo mitosis or apoptosis in response to adrenalectomy. *J. Comp. Neurol.* **369**: 56-63.

Carriere, R. (1967). Polyploidy cell reproduction in normal adult rat liver. *Exp. Cell Res.* **46**: 533-540.

Caviness, V.S. (1973). Time of neuron origin in the hippocampus and dentate gyrus of normal and reeler mutant mouse. *J. Comp. Neurol.* **151**: 235-254.

Celio, M.R. (1990). Calbindin D-28k and parvalbumin in the rat nervous system. *Neuroscience* **35**: 375-475.

Cleaver, J.E. (1967). *Thymidine Metabolism and Cell Kinetics.* North Holland Publishing Co., Amsterdam

Cogeshall, R.E., Jaksta, B.A., and Schwartz, F.J. (1970). A cytophotometric analysis of the DNA in the nucleus of the giant cell, R-2, in Aplysia. *Chromosoma* **32**: 205-212.

Cowan, W.M., Stanfield, B.B., and Kishi, K. (1980). The development of the dentate gyrus. *Curr. Topics in Dev. Biol.* **15**: 103-157.

Craig, C.G., Morshead, C.M., Roach, A. and van der Kooy, D. (1994). Evidence for a relatively quiescent stem cell in the adult mammalian forebrain. *J. Cell. Biochem.* **18**: (Suppl.), 176.

Crespo, D., Stanfield, B.B., and Cowan, W.M. (1986). Evidence that late-generated granule cells do not simply replace earlier formed neurons in the rat dentate gyrus. *Exp. Brain Res.* **63**: 195-204.

Eckenhoff, M.F. and Rakic, P. (1984). Radial organization of the hippocampal dentate gyrus: A golgi, ultrastructural and immunocytochemical analysis in the developing rhesus monkey. *J. Comp. Neurol.* **223**: 1-21.

Eckenhoff, M.F. and Rakic, P. (1988). Nature and fate of proliferative cells in the hippocampal dentate gyrus during the life span of the rhesus monkey. *J. Neurosci.* **8**: 2729-2747.

Feinendegen, L.E. (1967). *Tritium-labeled Molecules in Biology and Medicine*. Academic Press, New York. Chapter 6, pp. 309-353.

Fernandez, V. (1969). An autoradiographic study of the development of the anterior thalamic group and limbic cortex in the rabbit. *J. Comp. Neurol.* **136**: 423-452.

Fernandez, V., and Bravo, H. (1974). Autoradiographic study of the development of the cerebral cortex in the rabbit. *Brain Behav. Evol.* **9**: 317-332.

Fishell, G., Mason, C., and Hatten, M.E. (1993). Dispersion of neural progenitors within the germinal zones of the forebrain. *Nature* **362**: 636-638.

Gage, F.H., Coates, P.W., Palmer, T.D., Kuhn, H.G., Fisher, L.J., Suhonen, J.O., Peterson, D.A., Suhr, S.T., and Ray, J. (1995). Survival and differentiation of adult neuronal progenitor cells transplanted to the adult brain. *Proc. Nat. Acad. Sci. U.S.A.* **92**: 11879-11883.

Gall, C.N., Rose, G., and Lynch, G. (1979). Proliferation and migratory activity of glial cells in the partially deafferented hippocampus. *J. Comp. Neurol.* **183**: 539-550.

Ghandour, M.S., Langley, O.K., Labourdette, G., Vincendon, G. and Gombos,G. (1981a). Immunocytochemical and immunohistochemical study of S-100 protien: An astrocyte marker in rat cerebellum. *Dev. Neurosci.* **4**: 98-109.

Goldman, S.A. and Nottebohm, F. (1983). Neuronal production, migration, and differentiation in a vocal control nucleus of the adult female canary bird. *Proc. Nat. Acad. Sci. U.S.A.* **80**: 2390-2394.

Goss, R.J. (1967). *Control of the Cellular Growth in Adult Organisms.* Teir, J. and Rytomaa, T. (eds) Academic Press, New York. pp. 3-16.

Gould, E., Wooley, C.S., and McEwen, B.S. (1990). Short-term glucocorticoid manipulations affect neuronal morphology and survival in the adult dentate gyrus. *Neuroscience* **37**: 367-375.

Gould, E., Cameron, H.A., Daniels, D.C., Wooley, C.S., and McEwen, B.S. (1992). Adrenal hormones suppress cell division in the adult rat dentate gyrus. *J. Neurosci.* **12**: 3642-3650.

Gould, E. and McEwen, B.S. (1993). Neuronal birth and death. *Curr. Opin. Neurobiol.* **3**: 676-682.

Granzber, H.G. (1982). Monoclonal antibody to 5-bromo and 5-iododeoxyuridine: a new reagent for the detection of DNA replication. *Science* **218**: 474-475.

Gueneau, G., Privat,A., Drouet, J., and Court, L. (1982). Subgranular zone of the dentate gyrus of young rabbits as a secondary matrix. A high resolution autoradiographic study. *Dev. Neurosci.* **5**: 345-358.

Hajos, F. and Kalman, M. (1989). Distribution of glial fibrillary acidic protein (GFAP)-immunoreactive astrocytes in the rat brain. II. Mesencephalon, rhombencephalon and spinal cord. *Exp Brain Res.* **78**: 147-163.

Hanawalt, P.C., Cooper, P.K., Ganesan, A.K., and Smith, C.A. (1979). DNA repair in bacteria and mammalian cells. *Ann. Rev. Biochem.* **48**: 783-816.

Hebb, D.O. (1949). The Organization of Behavior: A Neuropsychological Theory. Wiley, New York.

Hine, R.J. and Das, G.D. (1974). Neuroembryogenesis in the hippocampal formation of the rat: An autoradiographic study. *Z. Anat. Entwickl.-Gesch.* **144**: 173-186.

Howard-Flanders, P. (1973). DNA repair and recombination. *Br. Med. Bull.* **29**: 226-231.

Hughes, W.L., Bond, V.P., Brecher, G., Cronkite, E.P., Painter, R.B., Quastler, H., and Sherman, F.G. (1958). Cellular proliferation in the mouse as revealed by autoradiography with tritiated thymidine. *Proc. Nat. Acad. Sci. U.S.A.* **44**: 476-483.

Isaacson, R.L. (1987). Hippocampus. In: Adelman G (ed) *Encyclopedia of Neurosciences*. vol. 1. Birkhauser, Basel. pp. 492-495.

Kaplan, [illegible]
microsc[illegible]

Korr, H. (1980). Prolif[illegible]
Embryol. Cell Biol. 61: 1-7[illegible].

Kosaka, T. and Hama, K. (1986)
rat dentate gyrus. J. Comp.

D.W., Egan, M.E.,
linear arrest and
17.

Kuhn, H.G., Dick
dentate gyrus
proliferation

Isaacson, R.L. and Pribram, K.H. (eds) (1975). *The Hippocampus.* vols. 1, 2. Plenum, NewYork.

Isaacson, R.L. and Pribram, K.H. (eds) (1985). *The Hippocampus.* vols. 3, 4. Plenum, New York.

Kalman, M. and Hajos, F. (1989). Distribution of glial fibrillary acidic protein (GFAP)-immunoreactive astrocytes in the rat brain. I. Forebrain. *Exp Brain Res.* **78**: 147-163.

Kaplan, M.S. and Bell, D.H. (1984). Mitotic neuroblasts in the 9-day-old and 11-month-old rodent hippocampus. *J. Neurosci.* **4**: 1429-1441.

Kaplan, M.S. and Hinds, J.W. (1977). Neurogenesis in the adult rat: Electron microscopic analysis of light radiographs. *Science* **197**: 1092-1094.

Korr, H. (1980). Proliferation of different cell types in the brain. *Adv. Anat. Embryol. Cell Biol.* **61**: 1-72.

Kosaka, T. and Hama, K. (1986). Three dimensional structure of astrocytes in the rat dentate gyrus. *J. Comp. Neurol.* **249**: 242-260.

Kufe, D.W., Egan, M.E., Rosowsky, A., Ensminger, W., and Frei, E. (1980). Thymidine arrest and synchrony of cellular growth in vivo. *Cancer Treat Rep.* **64**: 1307-1317.

Kuhn, H.G., Dickinson-Anson, H., and Gage, F.H. (1996). Neurogenesis in the dentate gyrus of the adult rat: Age-related decrease of neuronal progenitor proliferation. *J. Neurosci.* **16**: 2027-2033.

Kunkel, D.D., Lacaille, J-C. and Schwartzkroin, P.A. (1988). Ultrastructure of stratum lacunosum-moleculare interneurons of hippocampal CA1 region. *Synapse* **2**: 382-394.

Lapham, L.W., Lentz, R.D., Woodward, D.J., Hoffer, B.J., and Herman, C.J. (1971). Post-natal development of tetraploid DNA content in the Purkinje neuron of the rat: an aspect of cellular differentiation. *UCLA Forum in Medical Sciences.* **14**: 61-71.

Lasek, R. and Dower, W. (1971). Aplysia californica: analysis of nuclear DNA in individual nuclei of giant neurons. *Science* **172**: 278-280.

Lacaille, J-C., Kunkel, D.D. and Schwartzkroin, P.A. (1989). Electrophysiological and morphological characterization of hippocampal interneurons. In: The Hippocampus-New Vistas, Alan R. Liss, Inc., New York. pp.287-305.

Laurberg, S. (1979). Commisural and intrinsic connections of the rat hippocampus. *J. Comp. Neurol.* **184**: 685-708.

Leong, S. and Ling, E. (1992). Amoeboid and ramified microglia: Their response to brain injury. *Glia* **6**: 39-47.

Levitt, P. and Rakic, P. (1980). Immunoperoxidase localization of glial fibrillary acidic protein in radial glial cells and astrocytes of the developing rhesus monkey. *J. Comp. Neurol.* **193**: 815-840.

Lewis, P.D. (1978). Kinetics of cell proliferation in the postnatal rat dentate gyrus. *Neuropath. Appl. Neurobiol.* **4**: 191-195.

Lois, C. and Alvarez-Buylla, A. (1993). Proliferating subventricular zone cells in the adult mammalian forebrain can differentiate into neurons and glia. *Proc. Nat. Acad. Sci. USA* **90**: 2074-2077.

Lois, C. and Alvarez-Buylla, A. (1994). Long distance neuronal migration in the adult mammalian brain. *Science* **264**: 1145-1148.

Lorente de Nó, R. (1934). Studies on the structure of the cerebral cortex. II. Continuation of the study of the ammonic system. *J. Psychol. Neurol.* **46**: 113-177.

Matus, A. and Mughal, S. (1975). Immunohistochemical localization of S-100 protein in brain. *Nature* **258**: 746-748.

Maurer, H.R. (1981). Potential pitfalls of [^{3}H] thymidine techniques to measure cell proliferation. *Cell Tissue Kinet.* **14**: 111-120.

Mazur, E.M. (1990). Control and implications of polyploidization in human megakaryocytes. *Prog. Clin. Biol. Res.* **356**: 231-244.

McConnell, J.A. (1981). Identification of early neurons in the brainstem and spinal cord. II. An autoradiographic study in the mouse. *J. Comp. Neurol.* **200**: 273-288.

Medvedez, Z.A. (1986). Age-related polyploidization of hepatocytes: the cause and possible role. A mini-review. *Experimental Gerontology* **21**: 277-282.

Miller, M.W. and Nowakowski, R.S. (1988). Use of bromodeoxyuridine immunohistochemistry to examine the proliferation, migration, and time of origin of cells in the central nervous system. *Brain Res.* **457**: 44-52.

Morris, S.M. (1991). The genetic toxicology of 5-bromodeoxyuridine in mammalian cells. *Mutation Research* **258**: 161-188.

Morshead, C.M. and van der Kooy, D. (1992). Post-mitotic death is the fate of constituitively proliferating cells in the subependymal layer of the adult mouse brain. *J. Neurosci.* **13**: 2930-2938.

Morshead, C.M., Reynolds, B.A., Craig, C.G., McBurney, M.W., Staines, W.A., Morassutti, D., Weiss, S., and van der Kooy, D. (1994). Neural stem cells in

the adult mammalian forebrain: A relatively quiescent subpopulation of subependymal cells. *Neuron* **13**: 1071-1082.

Mullen, R.J., Buck, C.R., and Smith, A.M. (1992). NeuN, a neuronal specific nuclear protein in vertebrates. *Development* **116**: 201-211.

Naegeli, H. (1995). Mechanisms of DNA damage recognition in mammalian nucleotide excision repair. *FASEB* **9**: 1043-1050.

Nagl, W. (1990). Polyploidy in differentiation and evolution. *International Journal of Cell Cloning* **8**: 216-223.

Nornes, H.O. and Carry, H. (1978). Neurogenesis in the spinal cord of the mouse: an autoradiographic analysis. *Brain Res.* **159**: 1-16.

Nowakowski, R.S. and Miller, M.W. (1988). Use of bromodeoxyuridine immunohistochemistry to examine the proliferation, migration, and time of origin of cells in the central nervous system. *Brain Res.* **457**: 44-52.

Nowakowski, R.S., Lewin, S.B., and Miller, M.W. (1989). Bromodeoxyuridine immuno-histochemical determination of the lengths of the cell cycle and the DNA-synthetic phase for an anatomically defined population. *J. Neurocytology* **18**: 311-318.

Nowakowski, R.S. and Rakic, P. (1981). The site of origin and route and rate of migration of neurons to the hippocampal region of the rhesus monkey. *J. Comp. Neurol.* **196**: 129-154.

Olsson, L. (1976). Effects of tritium-labeled pyrimidine nucleosides on epithelial cell proliferation in the mouse. I. Cytodynamic perturbations in normal circadian rhythms after a single injection of ^{3}H-TdR. *Rad. Res.* **68**: 258-264.

O'Rourke, N.A., Dailey, M.E., Smith, S.J., and McConell, S.K. (1992). Diverse migratory pathways in the developing cerebral cortex. *Science* **258**: 299-302.

Packard, D.S., Menzies, R.A., and Skalko, R.G. (1973). Incorporation of thymidine and its analogue, bromodeoxyuridine, into embryos and maternal tissues of the mouse. *Differentiation* **1**: 397-405.

Perry, V.H., Hume, D.A., and Gordon, S. (1985). Immunohistochemical localization of macrophages and microglia in the adult and developing mouse brain. *Neuroscience* **15**: 313-326.

Pictet, R., Clark, W., Williams, K., and Rutter, W. (1972). An ultrastructural analysis of the developing embryonic pancreas. *Dev. Biol.* **29**: 436-467.

Rakic, P. (1985a). Limits of neurogenesis in primates. *Science* **227**: 154-156.

Rakic, P. (1985b). DNA synthesis and cell division in the adult primate brain. *Ann. NY Acad. Sci.* **456**: 193-211.

Rakic, P. and Nowakowski, R.S. (1981). The time of origin of neurons in the hippocampal region of the adult rhesus monkey. *J. Comp. Neurol.* **196**: 99-128.

Raza, A., Ucar, K., and Preisler, H.D. (1985). Double labeling and *in vitro* versus *in vivo* incorporation of bromodeoxyuridine in patients with acute nonlymphocytic leukemia. *Cytometry* **6**: 633-640.

Redman, R and Sreebny, L. (1970). Proliferative behavior of differentiating cells in the developing rat parotid gland. *J. Cell Biol.* **46**: 81-87.

Reznikov, K.Y. (1991). Cell proliferation and cytogenesis in the mouse hippocampus. *Adv. Anat. Embryol. Cell Biol.* **122**: 1-83.

Rose, G., Lynch, G., and Cotman, C.W. (1976). Hypertrophy and redistribution of astrocytes in the deafferented dentate gyrus. *Brain Res. Bull.* **1**: 87-92.

Rousselot, P., Lois, C., and Alvarez-Buylla, A. (1995). Embryonic (PSA) N-CAM reveals chains of migrating neuroblasts between the lateral ventricle and the olfactory bulb of adult mice. *J. Comp. Neurol.* **351**: 51-61.

Sawicki, W., and Dorn, A. (1973). Action of exogenous thymidine in vivo on progenitor cell cycle in intestinal epithelium. *Acta histochem.* **46**: 181-185.

Schlessinger, A.R., Cowen, W.M., Gottlieb, D.I. (1975). An autoradiographic study of the time and origin and pattern of granule cell migration in the dentate gyrus of the rat. *J. Comp. Neurol.* **159**: 149-176.

Schultze, B. and Korr, H. (1981). Cell kinetic studies of different cell types in the developing and adult brain of the rat and mouse: A review. *Cell Tissue Kinet.* **14**: 309-325.

Schwartzkroin, P.A. and Mathers, L.H. (1978). Physiological and morphological identification of a nonpyramidal hippocampal cell type. *Brain Res.* **157**: 1-10.

Schwerdtfeger, W.K. (1984). Structure and fiber connections of the hippocampus. *Adv. Anat. Embryol. Cell Biol.* **83**: 1-69.

Seki, T. and Arai, Y. (1995). Age-related production of new granule cells in the adult dentate gyrus. *NeuroReport* **6**: 2479-2482.

Sidman, R.L., Miale, I.L., and Feder, M. (1959). Cell proliferation and migration in the primitive subependymal zone; an autoradiographic study of histogenesis in the nervous system. *Exp. Neurol.* **1**: 322-333.

Sidman, R.L., Angevine, J.B. Jr, and Pierce, E.A. (1971). *Atlas of the Mouse Brain and Spinal Cord.* Harvard University Press. Cambridge.

Slotnick, B.M. and Leonard, C.M. (1975). A Stereotaxic Atlas of the Albino Mouse Forebrain. *Drew Publications*. Washington D.C.

Sloviter, R.S. (1989). Calcium-binding protein (calbindin-D-28k) and parvalbumin immunocytochemistry: localization in the rat hippocampus with specific reference to the selective vulnerability of hippocampal neurons to seizure activity. *J. Comp. Neurol.* **280**: 183-196.

Spector, R. (1980). Thymidine transport in the central nervous system. *J. Neurochem.* **35**: 1092-1098.

Spector,R. and Berlinger, W.G. (1982). Localization and mechanism of thymidine transport in the central nervous system. *J. Neurochem.* 39: 837-841.

Squire, L.R. (1992). Memory and the hippocampus: A synthesis of findings with rats, monkeys and humans. *Psychol. Rev.* **99**: 195-231.

Stanfield, B.B. and Cowan, W.M. (1979a). The morphology of the hippocampus and dentate gyrus in normal and reeler mice. *J. Comp. Neurol.* **185**: 393-422.

Stanfield, B.B. and Cowan, W.M. (1979b). The development of the hippocampus and dentate gyrus in normal and reeler mice. *J. Comp. Neurol.* **185**: 461-483.

Stanfield, B.B. and Trice, J.E. (1988). Evidence that granule cells generated in the dentate gyrus of adult rats extend axonal projections. *Exp. Brain Res.* **72**: 399-406.

Swanson, L.W., Wyss, J.M., Cowan, W.M. (1978). An autoradiographic study of the organization of intrahippocampal association pathways in the rat. *J. Comp. Neurol.* **181**: 681-716.

Taylor, J.H., Woods, P.S., and Hughes, W.L. (1957). The organization and duplication of chromosomes as revealed by autoradiographic studies using tritium-labeled thymidine. *Proc. Nat. Acad. Sci. U.S.A.* **43**: 122-128.

Trent, J.M., Gerner, R., Broderick, R., and Crossen, P.E. (1986). Cell cycle analysis using bromodeoxyuridine: comparison of methods for analysis of total cell transit time. *Cancer Genet.* **19**: 43-50.

Trice, J.E. and Stanfield, B.B. (1986). Evidence for the generation in the adult rat dentate gyrus of neurons which extend axonal projections. *Ann Neurol.* **20**: 392.

Troughton, W.D. and Trier, J.S. (1969). Paneth and goblet cell renewal in mouse duodenal crypts. *J. Cell Biol.* **41**: 251-268.

Waechter, R.V. and Jaensch, B. (1972). Generation times of the matrix cells during embryonic brain development: an autoradiographic study in rats. *Brain Res.* **46**: 235-250.

Walker, B. (1959). Polyploidy and differentiation in the transitional epithelium of the mouse urinary bladder. *Chromosoma* **9**: 105-118.

Winkelmann, M., Pfitzer, P., and Schneider, W. (1987). Significance of polyploidy in megakaryocytes and other cells in health and tumor disease. *Klin. Wochenschr.* **65**: 1115-1131.

Woodhams, E.B., Basco, E., Hajos, F., Csillag, A., and Balazs, R. (1981). Radial glia in the developing mouse cerebral cortex and hippocampus. *Anat. Embryol.* **163**: 331-343.

Wyss, J.M., and Sripanidkulchai, B. (1985). The development of Ammon's horn and fascia dentata in the cat: a [^{3}H]-thymidine analysis. *Dev. Brain Res.* **18**: 185-198.

Zimmer, J., and Sunde, N. (1984). Neuropeptides and astroglia in intracerebral hippocampal transplants: an immunohistochemical study in the rat. *J. Comp. Neurol.* **227**: 331-347.

Zola-Morgan, S., and Squire, L.R. (1993). Neuroanatomy of memory. *Ann. Rev. Neurosci.* **16**: 547-563.